

AERIAL SEED DISPERSAL SYSTEM

A Final Year Project Report

Presented to

SCHOOL OF MECHANICAL & MANUFACTURING ENGINEERING

Department of Mechanical Engineering

NUST

ISLAMABAD, PAKISTAN

In Partial Fulfillment
of the Requirements for the Degree of
Bachelor of Mechanical Engineering

by

Altamash Saqib

Muhammad Mehtab Asghar

Shuja Amjad

Tabsheer Ali Askari

June 2020

EXAMINATION COMMITTEE

We hereby recommend that the final year project report prepared under our supervision by:

ALTAMASH SAQIB	(175426)
MUHAMMAD MEHTAB ASGHAR	(188067)
SHUJA AMJAD	(177139)
TABSHEER ALI ASKARI	(190603)

Titled: “Aerial Seed Dispersal System” be accepted in partial fulfillment of the requirements for the award of Bachelor of Mechanical Engineering degree with grade ____

Supervisor: Dr.Yasar Ayaz(Associate Professor)	_____ Dated:
Committee Member: Dr. Muhammad Jawad Khan, (Assistant Professor)	_____ Dated:
Committee Member: Mr. Hamza Asif, (Lecturer)	_____ Dated:

(Head of Department)

(Date)

COUNTERSIGNED

Dated: _____

(Dean / Principal)

ABSTRACT

The aim of this project is to develop an Aerial Seed Drop System. It shall employ a quadcopter to drop a payload of Seedballs accurately and autonomously on locations which do not currently contain any trees and are suitable for plantation using image recognition. Moreover, the design focuses on harnessing the force of wind to provide additional range which facilitates proper germination of Seedballs. Unlike mechanisms currently in use around the world, it shall use the force of gravity and wind to simply drop, not fire, its payload.

ACKNOWLEDGMENTS

First and foremost, we thank Allah for having given us strength to undertake and carry out this project.

We are extremely grateful to our supervisor, Dr.Yasar Ayaz, for his continued support & encouragement. We would also like to thank Dr. Muhammad Jawad Khan for helping us with his experience and technical skills. We would like to thank Mr. Hamza Asif for his persistent guidance throughout the course of this project.

Last but not the least; we are indebted to our parents, without whom we would not have been able to achieve our goal.

ORIGINALITY REPORT

ORIGINALITY REPORT

5%

SIMILARITY INDEX

2%

INTERNET SOURCES

2%

PUBLICATIONS

4%

STUDENT PAPERS

PRIMARY SOURCES

1

[stackoverflow.com](#)

Internet Source

1%

2

[Submitted to Engineers Australia](#)

Student Paper

1%

3

[Jorge Castro, Alexandro B. Leverkus, Francisco Fuster. "A new device to foster oak forest restoration via seed sowing", New Forests, 2015](#)

Publication

<1%

4

[Submitted to University of New South Wales](#)

Student Paper

<1%

5

[Submitted to Taylors University College](#)

Student Paper

<1%

6

[Submitted to University of Leeds](#)

Student Paper

<1%

7

[Submitted to University of Nottingham](#)

Student Paper

<1%

8

[Submitted to Higher Education Commission Pakistan](#)

Student Paper

<1%

9	creativecommons.org Internet Source	<1%
10	Submitted to Plumpton College Student Paper	<1%
11	Submitted to City University Student Paper	<1%
12	Submitted to University of Strathclyde Student Paper	<1%
13	Submitted to Middle East Technical University Student Paper	<1%
14	Submitted to Emirates Aviation College, Aerospace & Academic Studies Student Paper	<1%
15	Submitted to North West University Student Paper	<1%
16	pubs.asha.org Internet Source	<1%
17	Submitted to Basaveshwar Engineering College (Autonomous) Vidyagiri Student Paper	<1%
18	Submitted to Southampton Solent University Student Paper	<1%
19	Submitted to Glasgow Caledonian University Student Paper	<1%

20 Submitted to Massachusetts Maritime Academy <1%
Student Paper

21 Michael K. Y. Fung. "FINANCIAL LIBERALIZATION AND ECONOMIC GROWTH: A THEORETICAL ANALYSIS OF THE TRANSFORMING CHINESE ECONOMY", Pacific Economic Review, 2/2005 <1%
Publication

22 docplayer.net <1%
Internet Source

23 Submitted to Galway-Mayo Institute of Technology <1%
Student Paper

24 Submitted to University of Hertfordshire <1%
Student Paper

25 openaccess.iyte.edu.tr <1%
Internet Source

26 Submitted to The Kilmore International School <1%
Student Paper

Exclude quotes Off

Exclude matches Off

Exclude bibliography On

TABLE OF CONTENTS

ABSTRACT	3
ACKNOWLEDGMENTS	4
ORIGINALITY REPORT	5
TABLE OF CONTENTS	8
LIST OF TABLES	12
LIST OF FIGURES	13
ABBREVIATIONS	16
NOMENCLATURE.....	17
CHAPTER 1: INTRODUCTION.....	19
Motivation.....	19
Problem Statement	19
Objectives	19
CHAPTER 2: LITERATURE REVIEW	20
CURRENT TREE PLANTATION METHODS	20
Manual Plantation	20
Seed Pouch Delivery	20

Aerial Seed Darts	21
Seed Dispersal Using a Fixed Wing UAV	21
Seed Bombs Using Helicopters	22
Pyramid Protection for Seeds.....	23
Multicopter-Based Seed Plantation.....	23
Seedballs	25
METHODS OF MULTICOPTER DEVELOPMENT.....	26
Hardware development and integration	26
Control of Multicopter	27
DECISION OF DISPERSAL MECHANISM TO EMPLOY	27
CHAPTER 3: METHODOLOGY	28
PAYLOAD (SEEDBALLS)	28
NEED FOR DISTANCE BETWEEN DROPS	28
DESIGN OF THE DISPERSAL MECHANISM	29
OPERATION	32
PIPE DESIGN.....	33
PARAMETRIC ANALYSIS	36
Projectile Motion	36
MOTOR SELECTION	37
BEARING SELECTION	37

SHAFT ANALYSIS	39
BOLT SELECTION AND ANALYSIS	40
FINITE ELEMENT ANALYSIS (FEA) OF MECHANISM.....	48
CONTROL ALGORITHM:.....	49
CHAPTER 4 RESULTS & CONCLUSIONS	51
CFD ANALYSIS	51
PARAMETRIC ANALYSIS	60
Projectile Motion:	60
MOTOR SELECTION	61
BEARING SELECTION	61
SHAFT ANALYSIS	62
BOLT SELECTION AND ANALYSIS	62
FINITE ELEMENT ANALYSIS	62
CONTROL ALGORITHM.....	66
DRONE MOTION SIMULATION	67
CHAPTER 5 CONCLUSION & RECOMMENDATIONS	68
REFERENCES.....	70
APPENDIX I: IMAGE PROCESSING CODE	73
APPENDIX II: EXIT VELOCITY MODEL	76

**APPENDIX III: MATLAB WORKSPACE VARIABLE DECLARATION
FOR SIMSCAPE MODEL77**

APPENDIX IV: SIMSCAPE MODEL79

LIST OF TABLES

Table 1: Properties of an Acacia modesta Seedball.....	28
Table 2: Mass of empty and loaded drop mechanism.....	30
Table 3: Loading conditions for Analysis.....	48
Table 4: Properties of PLA and Glass Fiber	48
Table 5: Drag coefficients for both tubes for sections shown in Figure 30.....	57
Table 6: Ball Exit Velocities and time in tube for different wind velocities	59
Table 7: Effect of wind and altitude on projectile range	61

LIST OF FIGURES

Figure 1: Seed Pouch (Courtesy: Wetzone Technologies LLC).....	20
<i>Figure 2: Aerial Seed Dart (Courtesy: The Forestry Chronicle 1984).....</i>	<i>21</i>
Figure 3: Seed Spreader Mount	22
Figure 4: (a) The seed shelter consists of two pyramids cut out of a 0.8 mm thick polypropylene sheet. (b) These pyramids (c) were linked at the base to form the protective structure, (d) which was filled with soil and an acorn and buried	23
Figure 5: Multicopter UAV based plantation (Courtesy: BioCarbon Engineering)	24
Figure 6: A broken out section of a Seedball.....	25
Figure 7: Intended Seedball drop technique	29
Figure 8: Isometric view of mechanism.....	30
Figure 9: Lateral View	30
Figure 10: The Seedball inlets to the 3 drop ramps (with outlet of directional sorter visible)	31
Figure 11: Initial Pipe Design	34
Figure 12: SG9g Mini Servo[12]	37
Figure 13: Analysis of load on Bearings Schematic[13]	38
Figure 14: Lateral view of Shaft	39
Figure 15: Cross-section of Shaft	39
Figure 16: Bolt Placements in Mechanism	40
Figure 17: Threaded Bolt Length[14]	41

Figure 18: Frustum of Joint Members[14].....	42
Figure 19: Control System Operation	49
Figure 20: Circuit Design (made on Fritzing, an opensource circuit design software)	50
Figure 21: Meshing for the region around and inside Drop Ramp	51
Figure 22: Velocity in x-axis for an Unnozzled Drop Ramp in a 4 m/s external flow field.....	52
Figure 23: Pressure Distribution for an Unnozzled Drop Ramp in a 4 m/s external flow field	52
Figure 24: Force Coefficients convergence plot for Seedball in Unnozzled Drop Ramp	53
Figure 25: Force Convergence Plot for Seedball in Unnozzled Drop Ramp.....	53
Figure 26: Velocity in x-axis for a Nozzled Drop Ramp in a 4 m/s external flow field.....	54
Figure 27: Pressure Distribution for a Nozzled Drop Ramp in a 4 m/s external flow field	55
Figure 28: Force Coefficients convergence plot for Seedball in Nozzled Drop Ramp	55
Figure 29: Force convergence plot for Seedball in Nozzled Drop Ramp.....	56
<i>Figure 30: (A) Drop tube without nozzle (side view), (B) Drop tube with nozzle (side view).</i>	
<i>Note that wind inlet is through the opening on left hand side and Seedball enters tube through the opening at the top.....</i>	<i>56</i>
Figure 31: Multiple views of ball travelling through drop ramp in a SIMSCAPE Multibody Simulation	58
Figure 32: 90-degree bend in tube made using 45 differential segments	59
Figure 33: Relation of Ramp Angle and Range of Projectile	60
Figure 34: Glass Fiber/PLA Glass Fiber Side.....	62

Figure 35: Glass Fiber/PLA PLA Side	63
Figure 36: PLA/PLA Top Side	63
Figure 37: PLA/PLA Bottom Side.....	64
Figure 38: PLA/PLA Top (Bottom Section).....	64
Figure 39: PLA/PLA Bottom (Bottom Section)	65
Figure 40: Stresses in Shaft.....	65
<i>Figure 41: (A) Raw Image taken by PiCamera, (B) Image Split into thirds for image processing</i>	<i>66</i>
Figure 42: Results of Image Processing, (A) Left Third, (B) Central Third, and (C) Right Third.....	67
Figure 43: : Simulating a drone flight path on SITL on ArduPilot.....	67

ABBREVIATIONS

CAD	Computer Aided Design
PLA	Polylactic Acid
RC	Remote Controller
UAV	Unmanned Aerial Vehicle

NOMENCLATURE

d	= Distance along ramp
A	= Frontal area of Seedball
c_d	= Drag coefficient of seed ball
m	= mass of seed ball
I	= Moment of inertia of seed ball
w	= Angular velocity
V_{ball}	= Linear Ball velocity
V_{wind}	= Wind speed
g	= Gravitational acceleration
h	= Vertical height
ρ	= Density of air
s	= Horizontal displacement of ball
H	= Drone flight altitude
v	= Ball exit velocity
t	= Time of flight of the seed ball
a_{xnet}	= Horizontal acceleration of Seedball
$a_{y net}$	= Vertical acceleration of Seedball
b	= Constant for projectile motion

Δx = Horizontal distance in one iteration

Δy = Vertical distance in one iteration

Δt = Time step of one iteration

V_x = Horizontal projectile velocity of ball

V_y = Vertical projectile velocity of ball

F_{rA}, F_{rB} = Radial Load of Bearing

C_{10} = Catalog Load Rating

f_w = Bearing Load Factor

K = Torsional Stiffness Constant

θ = Angle of Twist

T_{max} = Maximum Shear Stress

K_b = Bolt Stiffness

K_m = Member Stiffness

C = Fraction of external load carried by bolt

P = External Load

F_i = Pre-Load

S_p = Proof Strength

n = Load Factor

CHAPTER 1: INTRODUCTION

Motivation

Global warming is the most pressing problem of the 21st Century. Pakistan is among the top 10 countries most affected by climate change.[1] Therefore, steps to slow down Global Warming (such as large-scale tree plantation) must be taken with the utmost urgency. Existing seed plantation methods in the country are generally manual, slow and inefficient.

Drone based seeding is being used globally to increase productivity and reach of reforestation efforts. Such a solution is necessary in Pakistan since much of the terrain that is viable for plantation is not easily traversed by humans.

Problem Statement

This project will focus on the design and development of a Seedball¹ drop system integrated with a drone.

Objectives

The deliverables of the project are as follows:

1. Literature Review
2. Design of Aerial Seed Drop System
3. Development of Aerial Seed Drop System
4. Control of Aerial and Seed Drop Systems.

¹ See the section “Seedballs” in CHAPTER 2: LITERATURE REVIEW

CHAPTER 2: LITERATURE REVIEW

CURRENT TREE PLANTATION METHODS

There are two broad categories into which all tree plantation methods fall. The first is the growing of saplings in a nursery and once they have reached a certain age, to transplant them to their permanent habitat (such as in a forest). The second method is the direct delivery of seeds to their permanent habitat, so there is no relocation/transplantation after seed germination.

Manual Plantation

The traditional method to plant seeds/saplings is to do so manually. Either the seeds are planted into the soil, or seedlings from a nursery are planted. Manual plantation has drawbacks

Seed Pouch Delivery

A biodegradable pouch is dropped from a slow moving aerial system.[2]This pouch contains nutrients and the seed as is visible in Figure 1.

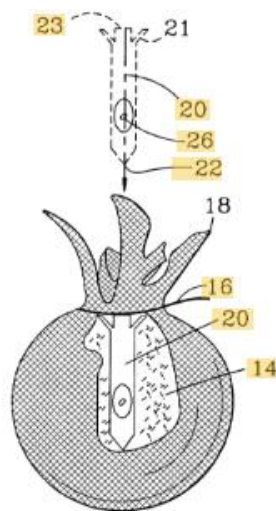


Figure 1: Seed Pouch (Courtesy: Wetzzone Technologies LLC)

There are two variations of this method. They are as follows:

1. A sharp stake is present inside the circular pouch which shall penetrate the pouch upon impact releasing the payload of the pouch.
2. In addition to method 1, the pouch may be made conical shaped. It shall contain nails that enhance pouch penetration into the soil.

Aerial Seed Darts

Paper-cone seed darts (See Figure 2) may be fired from a helicopter at various altitudes. This has been experimentally analyzed by Wood (1984).[3]

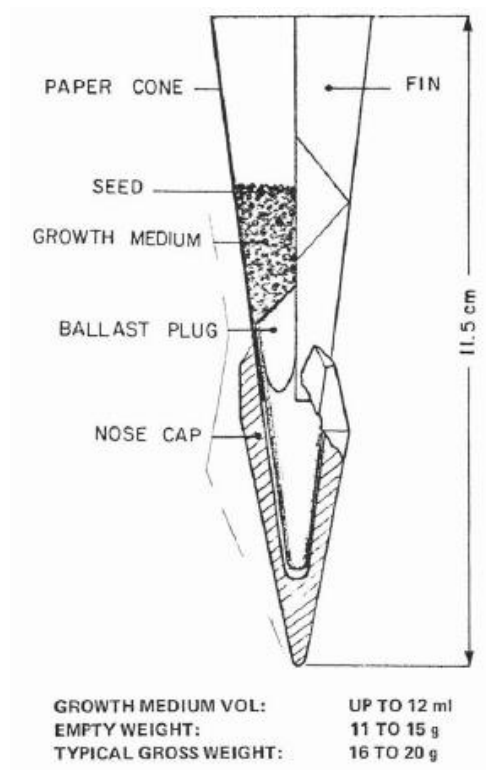


Figure 2: Aerial Seed Dart (Courtesy: The Forestry Chronicle 1984)

Seed Dispersal Using a Fixed Wing UAV

Mustafa Şahin et al. (2011) proposed and experimentally analyzed the use of a fixed wing UAV for throwing seeds using a rotary seed spreader mount on the base of the UAV (see Figure 3).

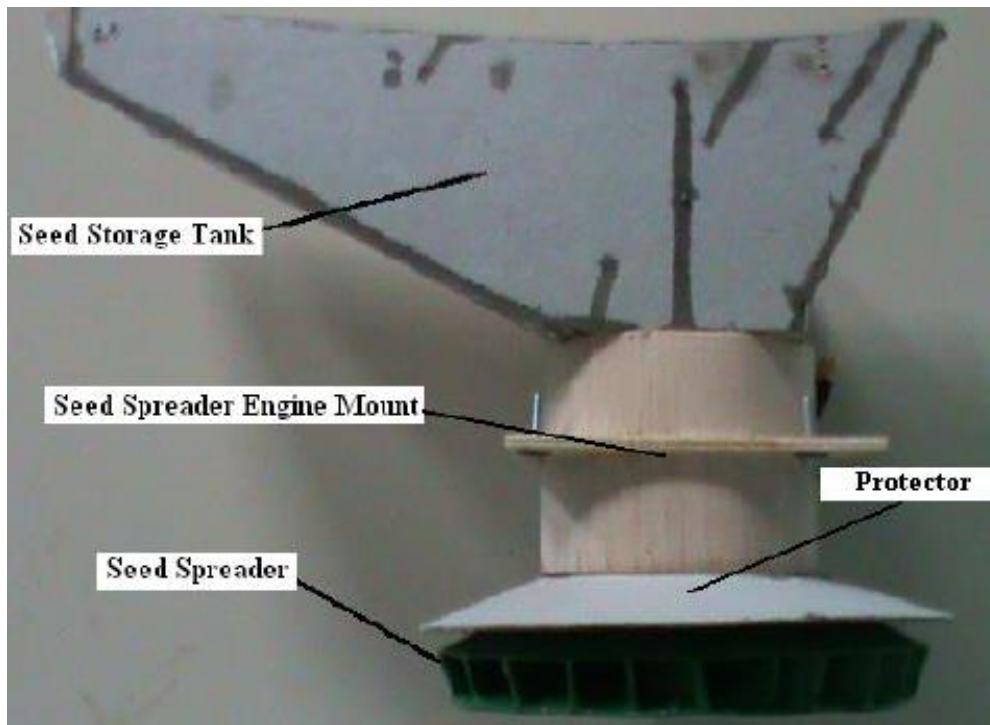


Figure 3: Seed Spreader Mount

Analysis included the variation in density of seed distribution, width of seed coverage and total area of seed coverage along the flight path of the UAV when aircraft ground speed, altitude of the aircraft and RPM of the mount were varied.[4]

The drawback to this was that a large percentage of seeds were wasted due to the inaccuracy of this broadcast seeding method². Also, plantation of unprotected seeds causes them to be more susceptible to damage from the elements, which reduces germination rate.[5]

Seed Bombs Using Helicopters

M. Ortolani et al. (2015) attempted throwing large seed bombs from a helicopter. These seed bombs were around 300g in mass and made of clay, with a seed at the center of the bomb. This method had very limited success since the bombs were prone to breakage upon impact with ground due to their bulky nature.[6]

²Broadcast seeding is a method of seeding that involves scattering seed, by hand or mechanically, over a relatively large area.

Pyramid Protection for Seeds

Another method employs a pyramidal vessel containing seeds which will allow the shoot to grow upward but will prevent animals from preying on the seeds.[7]

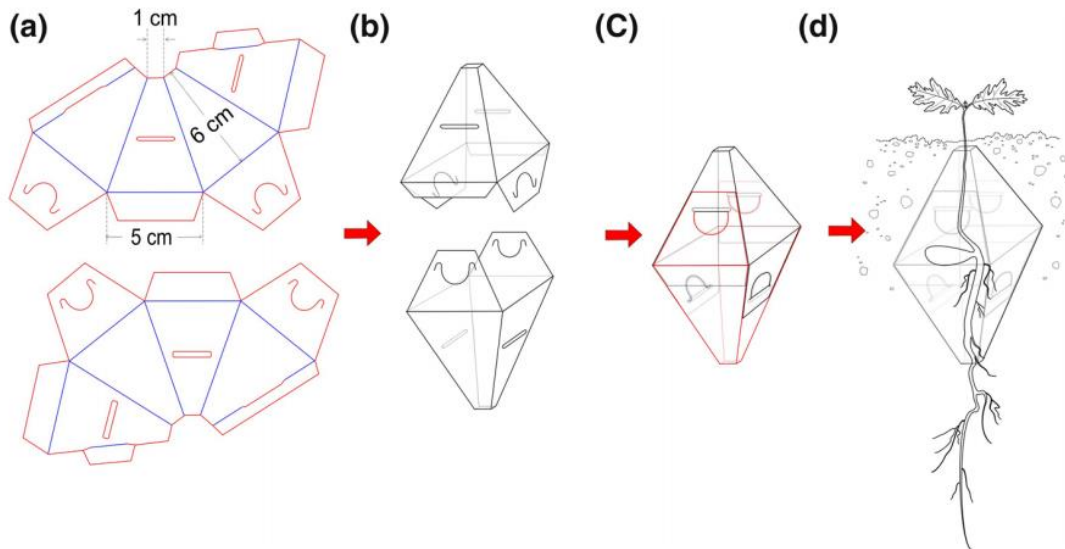


Figure 4.: (a) The seed shelter consists of two pyramids cut out of a 0.8 mm thick polypropylene sheet. (b) These pyramids (c) were linked at the base to form the protective structure, (d) which was filled with soil and an acorn and buried

This is designed specifically for acorns. Therefore, application for other species of seeds is unfeasible. Other than this, it needs to be placed into the ground, either manually or from slow moving ground-based vehicles, which severely limits the number of locations where it is applicable.

Multicopter³-Based Seed Plantation

In recent years, there has been an increasing trend towards multicopter-based plantation efforts. This is primarily a result of recent technological advances in multicopter technologies. Two companies that are leading this revolution are *DroneSeed* and *BioCarbon Engineering*. Their solutions have a very similar modus operandi, therefore in the course of this paper, they shall be treated as one method.

Theirs is a two-stage process. Firstly, fixed wing UAVs mounted with cameras fly across areas which may be viable for plantation. These UAVs map the area and identify

³ A multicopter is a rotary-wing aircraft that has more than two rotors.

microhabitats⁴ that would be the best for plantation. UAV multicopters are subsequently released on the site where they fire seed pods on the microhabitats that had been scoped out earlier. These seed pods are made up of a biodegradable polymer. They contain and protect the seed in the initial stages of germination. They also contain nutrients that help the seed during initial growth. The companies then provide follow-up UAV flights on the site to monitor germination success and to perform localized spraying of pesticides.[5]



Figure 5: Multicopter UAV based plantation (Courtesy: BioCarbon Engineering)

While this is a relatively advanced model for seed plantation, it has several drawbacks. The first and foremost is the need for mapping in advance by fixed-wing UAVs. Other than this, the seed pods need to fall vertically downward for effective soil penetration. In order to accomplish this, the drone needs to stop above every microhabitat, fire and resume on its flight path. This lowers the rate of plantation and necessitates the use of drone swarms to cover an area that could be covered by a single drone that did not stop periodically on the designated flight path.

⁴The definition of a microhabitat is a small specialized habitat within a larger habitat.

Seedballs

Effective success rate for direct seeding methods has remained low over the years. The main reason for this is simple: these methods are concerned only with depositing the seed at the habitat where it is to grow and not on protecting it against the elements and against predators. The Seedball addresses these issues well. This concept was initiated in Kenya by the company *Seedballs Kenya*, which is a joint collaborative between *Chardust Ltd* and *CookswellJikos*.

These balls are composed of a seed at the center which is surrounded by a dried layer of charcoal/clay and starch (see Figure 6). This outer layer serves several purposes. It protects the seed from the harsh environment that may be there at the time of plantation. It also deters predators from consuming the seed, since most predators are repelled by the clay and charcoal dust. It is dry; therefore, it prevents premature germination, keeping the seed dormant until the external conditions are favorable (such as when rainfall occurs). When the seed germinates, the charcoal and starch binder provide nutrients to facilitate growth.



Figure 6: A broken out section of a Seedball

However, as with other methods, Seedballs currently have several drawbacks. Most of the Seedball based plantation to date has been one of two types. The first type is where people scatter the Seedballs by hand. The second type is where they are scattered from low flying helicopters. Both methods are examples of Broadcast seeding. And as with all Broadcast seeding techniques, there is a large amount of Seed wastage (where seeds end up in microhabitats not appropriate for germination), overcrowding (where multiple seeds germinate in a small area, such that they are forced to over compete for nutrients) and the complete missing of microhabitats (where, due to the random nature of the dispersal technique, some suitable microhabitats have *no* seeds fall in them).

Moreover, with traditional manual plantation methods, the range of Seedball plantation is very limited. Humans are unable to traverse terrain that is difficult. Therefore, in areas with such terrain, traditional plantation is difficult. While Seedballs are a very viable initiative in themselves, there is dire need for automation in their dispersal techniques.

METHODS OF MULTICOPTER DEVELOPMENT

There are two parts to multicopter development.

1. Hardware development and integration,
2. Control of multicopter.

Hardware development and integration

Either an off the shelf drone can be acquired. Or the following components (that are compatible with each other) can be acquired:

1. DC Brushless Motors
2. Propellers
3. Electronic Speed Controllers (ESCs)
4. Frame
5. Flight controller (if intending to use an autopilot software) / Microcontroller (if intending to code own control software)
6. Battery
7. GPS Module

For this project, the second option (Self Assembly) has been considered in order to decrease cost of the Multicopter. A tradeoff is the additional work that must be done to assemble the Multicopter.

Control of Multicopter

This can be done in one of several ways:

1. Through an RC Controller (manual control),
2. Programming an *Arduino* or *Raspberry Pi* microcontroller for flight control,
3. Using a preprogrammed flight controller such as *Pixhawk* or *APM* and controlling the multicopter through autopilot software such as *Mission Planner*.

The third way (Pixhawk) will be used in this project since it provides most accurate control with minimum technical effort (simple plug and play configuration).

The multicopter type to be used is a quadcopter since it provides both high lift and accurate control.

DECISION OF DISPERSAL MECHANISM TO EMPLOY

Considering the literature review conducted on the seed dispersal mechanisms available, the best course of action will be to use Seedballs, due to the several reasons discussed above. In order to counteract the drawbacks of manual Seedball dispersal techniques, a multicopter-mounted automated dispersal mechanism is to be used. This increases dispersal range and accuracy. An autonomous quadcopter controlled by *Pixhawk* through *Mission Planner* shall be used as the vehicle upon which a gravity driven dispersal mechanism is mounted. The mechanism will simply drop, not fire the Seedballs, so that it needs less power and requires a smaller battery to operate.

One of the primary restrictions of quadcopter usage is the payload capacity. Therefore, mass of the mechanism must be minimal.

CHAPTER 3: METHODOLOGY

PAYLOAD (SEEDBALLS)

For the purpose of this project, Seedballs have been acquired from the Islamabad Chamber of Commerce and Industry (ICCI), where they are manufactured as part of a Corporate Social Responsibility (CSR) project. The following species of Seedballs are available:

1. Vachellianilotica (locally called Keekar)
2. Acacia modesta (locally called Phulai)
3. Cassia fistula (locally called Amaltas)

Acacia modesta has been used since it is indigenous to the Islamabad biome and is suitable for widespread plantation in most areas.[8]

The properties of this Seedball are given in Table 1.

Table 1: Properties of an Acacia modesta Seedball

Mass	12 g
Diameter	30 mm

NEED FOR DISTANCE BETWEEN DROPS

According to the Kansas Forest Service, responsible for managing Forestry and Horticulture in the US state of Kansas, Small Deciduous Trees grow best when the distancing between consecutive trees is 5-8 feet (1.52-2.44 m)[9]. At this distance, the forest cover is the maximum it can be without adverse effect on the growth of individual trees. All tree species we have listed in Methodology: Payload (Seedballs) are small Deciduous species.

Therefore, for our application, we aim for an optimum inter-tree distance of 2 m, as illustrated in the figure below.

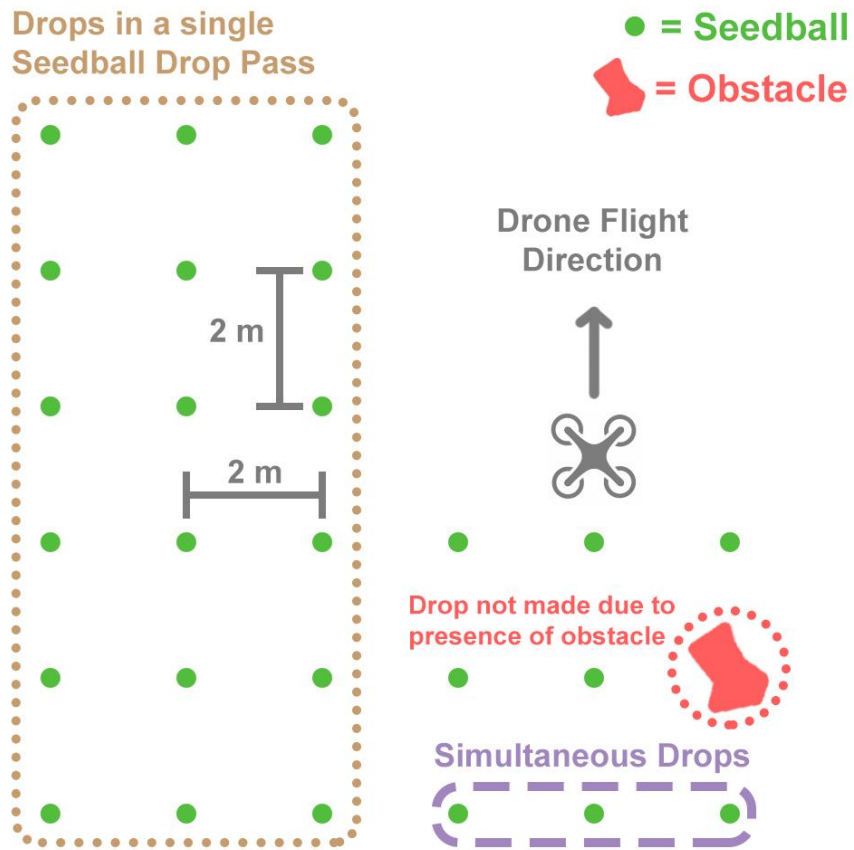


Figure 7: Intended Seedball drop technique

DESIGN OF THE DISPERSAL MECHANISM

The CAD model of the drop mechanism is shown in Figures 8 and 9.

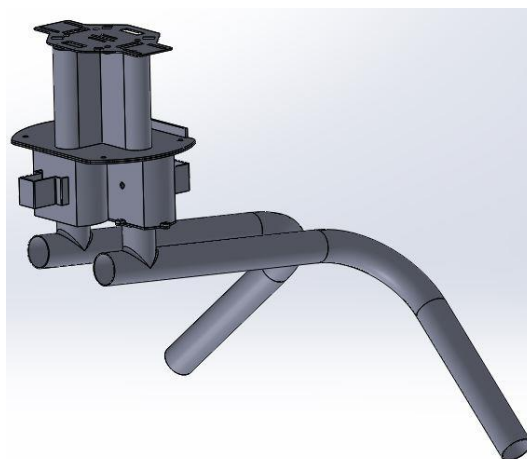


Figure 8: Isometric view of mechanism

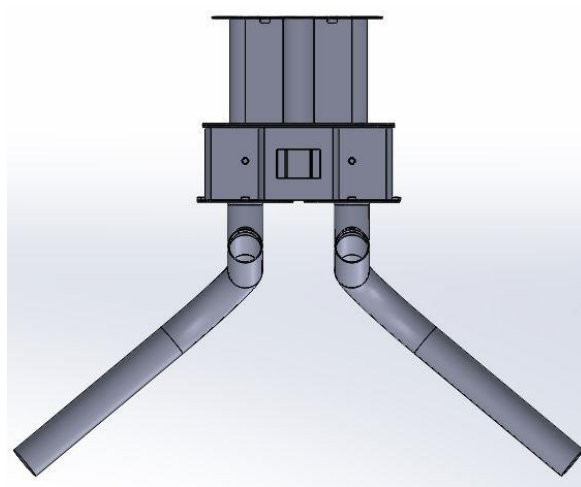


Figure 9: Lateral View

The height of the mechanism was 480 mm and the length of the sides was 594 mm.

Mass Calculations were done using SOLIDWORKS Mass Properties. The results are tabulated in Table 2.

Table 2: Mass of empty and loaded drop mechanism

Mass of drop mechanism without Seedballs	656.30 grams
Mass of 15 Seedballs	180 grams
Mass of electronics on Mechanism	390 grams
Total Mass of Mechanism	1226.3 grams

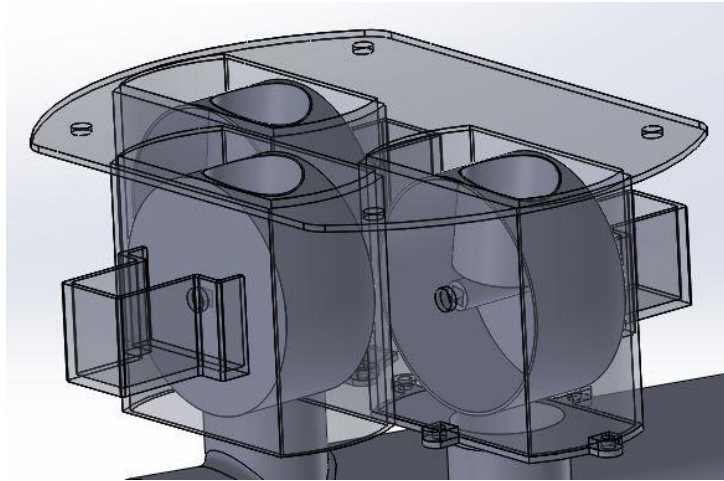


Figure 10: The Seedball inlets to the 3 drop ramps (with outlet of directional sorter visible)

The dispersal mechanism consists of the following main components (starting from the top, moving downward):

- Feed Hopper

This part shall store the Seedballs. It will have an inlet at the top for loading. It will have 3 outlets at the bottom, sized such that it allows a single Seedball to exit at a time. The current model of the feed hopper will contain at least 15 Seedballs.

- Loading Wheel

When a Seedball needs to be dropped, it will move from the hopper to the loading wheel due to the rotation of the wheel. The loading wheel will rotate a half revolution, to dump the Seedball onto their respective pipes below. The wheel is operated by a servo motor.

- Drop Ramps

There are three drop ramps. one of them leads vertically downward, the second is sloped towards the left and the third is sloped towards the right. The angle of inclination is 40 degrees below the horizontal.

If the Seedball falls into the vertical ramp, it will be dropped vertically downward. If it falls onto one of the other two ramps, it will roll down the slope of the ramp, by the forces of gravity and air pushing force⁵. It will be released such that it falls a short distance to the side of the quadcopter.

⁵ See air-assisted drop in OPERATION.

The priority was to manufacture these parts from carbon fiber, due to its high strength and low density, but due to financial restraints, we have shifted to 3D printing using Polylactic Acid (PLA) filament.

The drop mechanism was mounted to the frame of the quadcopter using 4 bolts on a base plate. The frame is made of glass fiber. Load analysis and FEA of the baseplate is given later in this report.

As well as electrical components that include:

- The Battery
- The Raspberry Pi
- Three Motors (For each of the landing wheels)
- Camera (for image recognition)

OPERATION

Before flight, the satellite imagery of the required area will be assessed, and a flight path will be generated for the drone on *Mission Planner*. This flight path will include way points where seeding is viable (areas with limited vegetation). This flight path shall be uploaded onto the flight controller. The drone will take off and approach the quadrant in which seeding is to be done. Throughout the flight, the drone shall be guided by the onboard GPS module.

The on-board camera shall use image processing to identify whether any drop locations are within range of the drop mechanism. Each time a location comes within range, the program will decide whether to drop the Seedball from the right, left or downward drop tube (or multiple tubes). This shall be repeated throughout the course of the designated flight path.

There were two methods considered for the dropping the Seedballs. They are as follows:

Simple Drop

The initial technique used was to drop the Seedball onto a drop ramp. It would roll down the ramp by the component of the gravitational force on it that was along the slope of the ramp.

Air-Assisted Drop

Since there is a range limitation when simply dropping the Seedballs from a ramp, an air assisted drop technique is used to increase range.

This solution works by harnessing the air around the Quadcopter through an inlet pipe and using the velocity of the Quadcopter relative to the freestream of air around it to impart a pushing force on the Seedball when it falls into one of the drop ramps. This is in addition to the gravitational force acting on it and gives it a greater horizontal velocity upon release from the drop tubes. Considering the clear advantage this mechanism has, it has been adopted.

PIPE DESIGN

Our first iteration of the pipe design was done on the basis of the horizontal displacement of the ball that we required. We initially assumed the altitude at which we would fly the drone. We then calculated the exit velocity of the ball and the angle of release that will displace the ball to the required distance. In order to minimize the exit velocity, we had to optimize the angle of exit of the ball so that maximum horizontal distance could be achieved. To do this, we employed MATLAB to plot a graph of the horizontal distance of the ball against the angle of release to get a point of maximum displacement. This angle was found to around 40 degrees, hence the slope of the pipe was chosen. The length of the pipe was then chosen according to the exit velocity that we required by substituting that velocity in the following mathematical model:

$$V_{ball} = \sqrt{\frac{10}{7} * g * h}$$

This model was verified in SIMSCAPE (MATLAB) by dropping a ball in our chosen pipe dimensions and inclination. The exit velocity of the ball from the simulation matched this model.



Figure 11: Initial Pipe Design

In order to enhance the displacement of the seed balls we used relative wind speed to increase the exit velocity of the ball. The drone would be flown against the direction of wind and the air intake by the mechanism will be utilized to push the seed ball. This will be useful in cases where there is an obstacle at the designated drop point, and we need an extra push to increase the ball velocity. In such cases we cannot change the inclination angle to enhance the horizontal displacement of the ball because that angle is already optimized (40 degrees) and it gives us maximum horizontal distance. Our first iteration of the pipe design is shown above.

When we added the wind force to the SIMSCAPE model, the exit velocity of the ball did not change significantly (an increase of 0.01 m/s was achieved). This was due to the lack of contact time between the ball and the wind force (approximately 0.3 sec). So, in order to enhance the effect of the wind speed, we increased the contact time by adding a long horizontal pipe at the entrance which would allow the ball to gain momentum from the incoming wind and thereby increasing its velocity when it enters the pipe and hence increasing the ball exit velocity.

The model governing this motion is:

$$\text{Energy in} = \text{Energy out}$$

$$\text{Relative wind energy} = \text{Friction} + \text{Linear K.E} + \text{Rotational K.E}$$

$$\left(c_d * \frac{1}{2} * \rho * (V_{wind} - V_{ball})^2 * A\right) * d = \frac{1}{2} * I * \omega^2 + \frac{1}{2} * m * V_{ball}^2$$

In the above equation, we have neglected frictional losses as they are negligible because of the low coefficient of friction between the ball and the pipe surface.

Seed ball exit velocity and the time taken by a seed ball to exit the pipe was calculated for different pipe lengths and a length was chosen which would cause the maximum allowable delay before the ball entering the ramp. This “delay time” was evaluated by dividing the distance between two consecutive plantations and the drone velocity.

Bend Radius

In the initial design, the bend was very sharp (having a mean radius of curvature of 2 cm) . This posed two problems:

1. The major head losses resulting from the sharp bend greatly lowered the air velocity inside the pipe. As a result, drag force on the Seedball when it was inside the pipe was also reduced. (Observed through CFD simulations on Simscale). Due to this, the wind assistance to the drop that was the purpose of the whole design was not being achieved properly.
2. If the Seedball achieved some velocity in the horizontal section, the resulting momentum would prevent it from following the contour of the sharp bend. It would instead collide with the outer surface of the bend. The inelastic nature of these collisions (Seedball to tube interactions were found to have a coefficient of restitution of 0.48 through experimentation) would reduce the velocity of the Seedball. This was extremely counterproductive, since the aim was to achieve maximum exit velocity of the Seedball.

Due to the reasons highlighted above, it was imperative to increase the radius of curvature of the bend. It was subsequently increased to a mean value of 10 cm. At this value, the head losses were low enough to allow a significant drag-based propulsion force to act on the Seedball. The velocity losses in the bend were also reduced, making the wind-assistance to the drop much more efficient.

As a result of the new design, we were able to enhance the exit velocity.

Nozzle Design

In order to enhance wind force, a design of nozzle was perceived and analyzed using CFD. Its results will be presented in the results section of the report. The nozzle was designed to minimize frictional losses and different variants of nozzles were tested to get the ideal most nozzle[10] was used to design the nozzle. The book contained different graphs of drag coefficients based upon the various dimensions of the nozzle which were used to design the nozzle.

Counteracting Pitching Effects of Drone During Operation

The horizontal section of the drop ramps is inclined 5 degrees below the horizontal on the downwind side. This is to counteract the effect of the pitching of the drone during flight, since the entire assembly pitches 3-4 degrees downward on the front side of the drone. The incline of the tubes in the opposite direction ensures that the Seedball will not fall out from the wind inlet. (See Drone Motion Simulation in Results)

PARAMETRIC ANALYSIS

Projectile Motion

A projectile motion model was developed on MATLAB to find the ranges of the Seedballs on the ground, given the ramp length, angle, altitude, relative velocity of quadcopter. The following equations[11] were used to calculate the required parameters using an iterative solver.

$$\vec{a}_{x_{net}} = -b|\vec{v}|^2 \cdot \hat{v}_x$$

$$\vec{a}_{y_{net}} = \vec{g} - b|\vec{v}|^2 \cdot \hat{v}_y$$

$$\vec{a}_{y_{net}} = g - b \cdot \sqrt{1 + \frac{v_x^2}{v_y^2}} \cdot v_y^2$$

$$\Delta v_y = g\Delta t - b \cdot \sqrt{v_x^2 + v_y^2} \cdot v_y \Delta t$$

$$\Delta v_x = -b \cdot \sqrt{v_x^2 + v_y^2} \cdot v_x \Delta t$$

$$\Delta x = v_x \cdot \Delta t + \frac{1}{2} \vec{a}_{x_{net}} \Delta t^2$$

$$\Delta y = v_y \cdot \Delta t + \frac{1}{2} \vec{a}_{y_{net}} \Delta t^2$$

This model incorporated the effect of air resistance and drag.

MOTOR SELECTION

Mass of seed ball = 12g

Torque Length = 3cm

Factor of Safety = 5

Torque = Mass of seed ball × Torque Length × Factor of Safety

Torque = **0.18 kgcm**

Hence,

We use *SG9g Mini Servo* as it provides *0.6 kgcm* [12] stall torque.



Figure 12: SG9g Mini Servo[12]

BEARING SELECTION

Weight of seed ball = 0.118N

Factor of Safety = 5

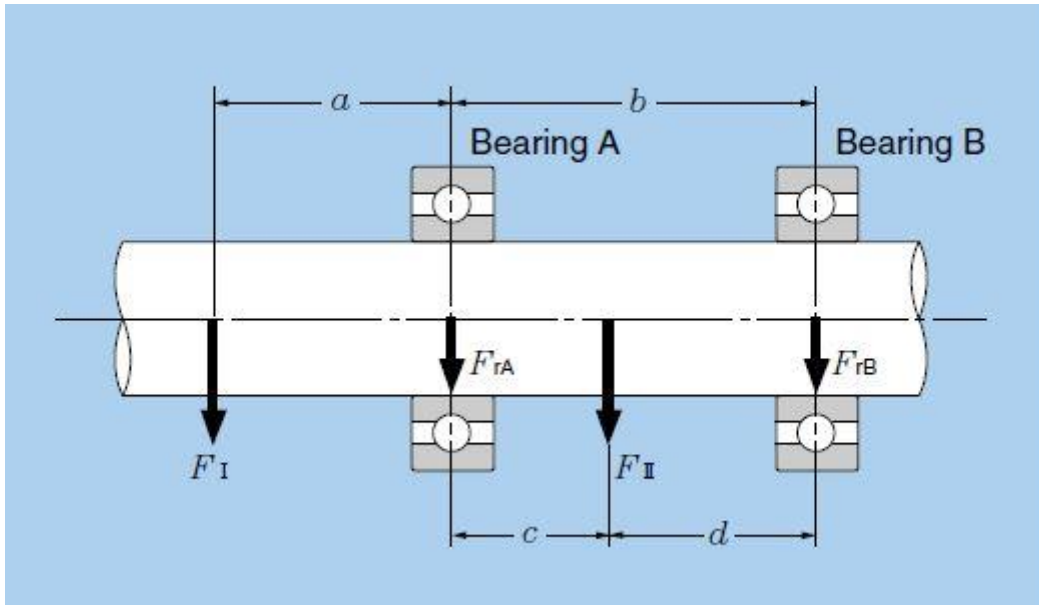


Figure 13: Analysis of load on Bearings Schematic[13]

According to our design,

$$F_I = 0$$

$$a = 0$$

$$F_{2w} = \text{Weight of seed ball} \times \text{Factor of Safety}$$

$$F_{2w} = 0.5886\text{N}$$

$$F_2 = f_w \times F_{2w} \text{ [12]}$$

$$f_w = 1.2$$

$$F_2 = 0.706\text{N}$$

$$F_{rA} = \frac{d}{c+d} F_2 \text{ [13]} \quad F_{rB} = \frac{c}{c+d} F_2 \text{ [13]}$$

$$c = d$$

$$F_{rA} = F_{rB} = \frac{F_2}{2} = 0.3532\text{N}$$

There is no axial thrust in the design.

Assumptions:

- Choosing bearing from SKF catalogue; $L_{10} = 10^6$ revolutions.
- Choosing bearing from single row deep groove ball bearing; $a = 3$

- Desired Life = $L_{DN_D} = 5000 \text{ hours} \times 1725 \text{ rev/min}$.
- Reliability = 90%

$$C_{10} = F_{rA} \left(\frac{L_D n_D \times 60}{L_{10}} \right)^{1/a} \quad [14]$$

$$C_{10} = 2.84 \text{ N}$$

Inner bore diameter = 5mm

We use **618/5**[15] single row deep groove ball bearing-SKF as its specs are:

$$C_{10} = 468 \text{ N}$$

Inner diameter = 5mm.

Outer diameter = 11mm.

Thickness = 3mm.

SHAFT ANALYSIS

Shaft was designed according to our requirement. Calculations are done to check whether shaft can bear the applied load, so shear stress is calculated which acts on the shaft and is compared with tensile strength of PLA.

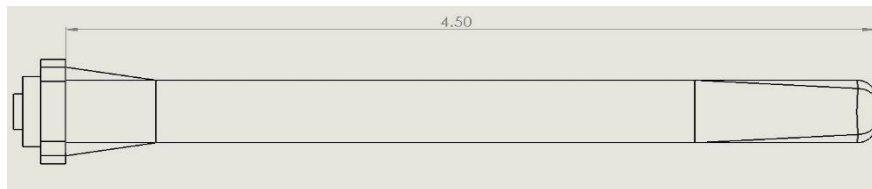


Figure 14: Lateral view of Shaft

$$\text{Torque} = T = 0.18 \text{ kgcm} = 0.01765 \text{ Nm}$$

$$\text{Length of shaft} = L = 4.5 \text{ cm}$$



Figure 15: Cross-section of Shaft

$$\text{Shear Modulus of PLA} = G = 2.4 \text{ GPa}$$

$$\text{Tensile Strength of PLA} = 37 \text{ MPa}$$

$$2a = 0.42 \text{ cm}$$

Hence,

$$\theta = \frac{TL}{KG} [16]$$

where,

$$K = 2.25a^4$$

$$K = 43.758 \text{ mm}^4$$

$$\theta = 0.008 \text{ radian}$$

$$T_{max} = \frac{0.601T}{a^3} [16]$$

$$T_{max} = 1.145 \text{ MPa}$$

As,

$$\text{Tensile Strength} > T_{max}$$

So, shaft cannot shear. As PLA is a brittle material, it will not bend.

BOLT SELECTION AND ANALYSIS

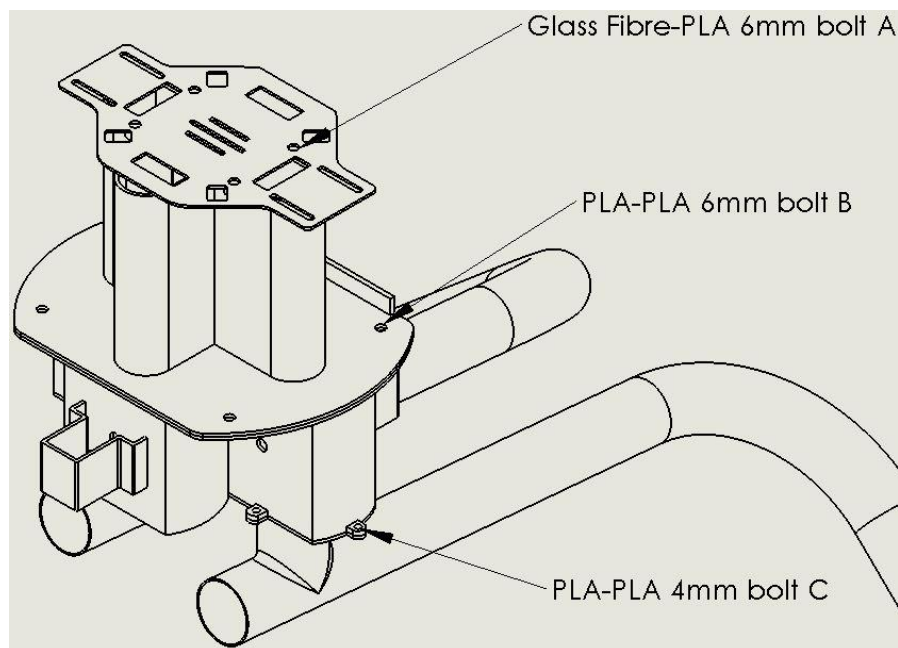


Figure 16: Bolt Placements in Mechanism

Glass Fiber-PLA 6mm bolt A

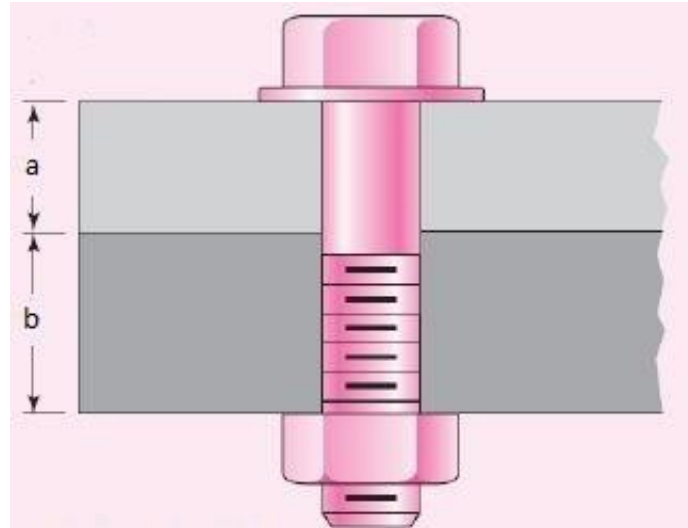


Figure 17: Threaded Bolt Length[14]

From Figure 17;

a (glass fiber) = 1.5mm

b (PLA) = 5mm

Grip length = $l = 6.5\text{mm}$

Nut Height = 5.2mm

Thread Pitch = 1mm

Using fully threaded bolt i.e. $L_D = 0$; $L_T = L$

Having 2 threads out of nut;

Length of bolt = $l = 13.7\text{mm}$

Hence using Bolt A = L = 14mm (standard size) [17]

Bolt Stiffness:

using steel bolts;

$$E = 207\text{GPa}$$

$$A_t = 20.1\text{mm}^2$$

$$K_b = \frac{A_t E}{L} [14]$$

$$K_b = 297.2 \text{ MN/m}$$

Member Stiffness:

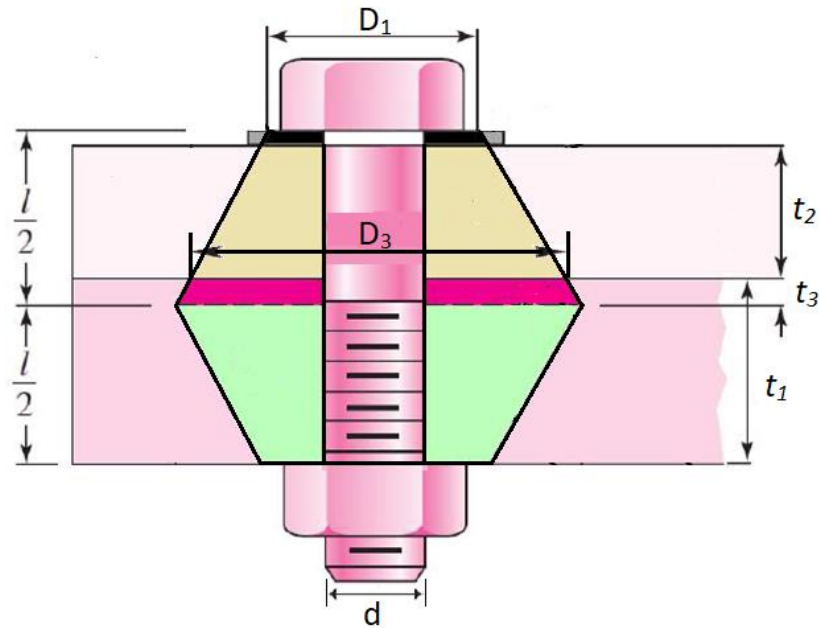


Figure 18: Frustum of Joint Members[14]

From Figure 18;

$$t_1 = 3.25\text{mm}$$

$$t_2 = 1.5\text{mm}$$

$$t_3 = 1.75\text{mm}$$

$$d = 6\text{mm}$$

$$D_1 = D_2 = 9\text{mm}$$

$$D_3 = 10.73\text{mm}$$

$$E_1 = E_3 = 2.89 \text{ GPa}$$

$$E_2 = 72 \text{ GPa}$$

As,

$$K_{mi} = \frac{0.5774\pi E_i d}{\ln\left[\frac{(1.155t_i + D_i - d)(D_i + d)}{(1.155t_i + D_i + d)(D_i - d)}\right]} \quad [14]$$

$$K_{m1} = 51.63 \text{ MN/m}$$

$$K_{m2} = 2261.3 \text{ MN/m}$$

$$K_{m3} = 130.11 \text{ MN/m}$$

$$\frac{1}{K_m} = \frac{1}{K_{m1}} + \frac{1}{K_{m2}} + \frac{1}{K_{m3}}$$

$$K_m = 36.37 \text{ MN/m}$$

$$C = \frac{K_b}{K_b + K_m} \quad [14]$$

$$C = 0.89$$

$$P = 10.8 \text{ N}$$

$$S_P = 225 \text{ MPa} \quad [14]$$

$$F_i = 0.75 \times A_t \times S_P \quad [14]$$

$$F_i = 3391.875 \text{ N}$$

$$\text{No. of bolts} = N = 4$$

$$n = \frac{S_P A_t - F_i}{C(P/N)} \quad [14]$$

$$\mathbf{n = 470.5}$$

as,

$\mathbf{n > 1}$, it ensures that bolt stress is less than proof strength so these bolts would not fail.

PLA-PLA 6mm bolt B

From Figure 18;

$$a \text{ (PLA)} = 2\text{mm}$$

$$b \text{ (PLA)} = 2\text{mm}$$

$$\text{Grip length} = l = 4\text{mm}$$

$$\text{Nut Height} = 5.2\text{mm}$$

$$\text{Thread Pitch} = 1\text{mm}$$

Using fully threaded bolt i.e. $L_D = 0$; $L_T = L$

Having 2 threads out of nut;

Length of bolt = $l = 11.2\text{mm}$

Hence using *Bolt B = L = 12mm* (standard size) [17]

Bolt Stiffness:

using steel bolts;

$$E = 207\text{GPa}$$

$$A_t = 20.1\text{mm}^2$$

$$K_b = \frac{A_t E}{L} \text{ [14]}$$

$$K_b = 346.73 \text{ MN/m}$$

Member Stiffness:

From Figure 16;

$$t_1 = t_2 = 2\text{mm}$$

$$t_3 = 0\text{mm}$$

$$d = 6\text{mm}$$

$$D_1 = D_2 = 9\text{mm}$$

$$D_3 = 0\text{mm}$$

$$E_1 = E_2 = 2.89 \text{ GPa}$$

As,

$$K_{mi} = \frac{0.5774\pi E_i d}{\ln\left[\frac{(1.155t_i + D_i - d)(D_i + d)}{(1.155t_i + D_i + d)(D_i - d)}\right]} \text{ [14]}$$

$$K_{m1} = K_{m2} = 73.53 \text{ MN/m}$$

$$\frac{1}{K_m} = \frac{1}{K_{m1}} + \frac{1}{K_{m2}}$$

$K_m = 36.8\text{MN/m}$, Hence

$$C = \frac{K_b}{K_b + K_m} [14]$$

$$C = 0.904$$

$$P = 8.94 \text{ N}$$

$$S_P = 225 \text{ MPa [14]}$$

$$F_i = 0.75 \times A_t \times S_P$$

$$F_i = 3391.875 \text{ N}$$

$$\text{No. of bolts} = N = 4$$

$$n = \frac{S_P A_t - F_i}{C(P/N)}$$

$$\mathbf{n = 559.59}$$

as,

$\mathbf{n > 1}$, it ensures that bolt stress is less than proof strength so these bolts would not fail.

PLA-PLA 4mm bolt C

From Figure 18;

$$a \text{ (PLA)} = 3\text{mm}$$

$$b \text{ (PLA)} = 2\text{mm}$$

$$\text{Grip length} = l = 5\text{mm}$$

$$\text{Nut Height} = 3.2\text{mm}$$

$$\text{Thread Pitch} = 0.7\text{mm}$$

Using fully threaded bolt i.e. $L_D = 0$; $L_T = L$

Having 2 threads out of nut;

Length of bolt = $l = 9.6\text{mm}$

Hence using Bolt $C = L = 10\text{mm}$ (standard size) [17]

Bolt Stiffness:

using steel bolts;

$$E = 207\text{GPa}$$

$$A_t = 8.78\text{mm}^2$$

$$K_b = \frac{A_t E}{L}$$

$$K_b = 181.75 \text{ MN/m}$$

Member Stiffness:

From Figure 16;

$$t_1 = 2\text{mm}$$

$$t_2 = 2.5\text{mm}$$

$$t_3 = 0.5\text{mm}$$

$$d = 4\text{mm}$$

$$D_1 = D_2 = 6\text{mm}$$

$$D_3 = 8.309\text{mm}$$

$$E_1 = E_2 = E_3 = 2.89 \text{ GPa}$$

As,

$$K_{mi} = \frac{0.5774\pi E_i d}{\ln \left[\frac{(1.155t_i + D_i - d)(D_i + d)}{(1.155t_i + D_i + d)(D_i - d)} \right]}$$

$$K_{m1} = 32.77 \text{ MN/m}$$

$$K_{m2} = 37.45 \text{ MN/m}$$

$$K_{m3} = 262.38 \text{ MN/m}$$

$$\frac{1}{K_m} = \frac{1}{K_{m1}} + \frac{1}{K_{m2}} + \frac{1}{K_{m3}}$$

$K_m = 16.38 \text{ MN/m}$, Hence

$$C = \frac{K_b}{K_b + K_m}$$

$$C = 0.917$$

$$P = 0.36 \text{ N}$$

$$S_P = 310 \text{ MPa}[14]$$

$$F_i = 0.75 \times A_t \times S_P$$

$$F_i = 2041.35 \text{ N}$$

$$\text{No. of bolts} = N = 4$$

$$n = \frac{S_P A_t - F_i}{C(P/N)}$$

$$\mathbf{n = 8244.88}$$

as,

$\mathbf{n > 1}$, it ensures that bolt stress is less than proof strength so these bolts would not fail.

FINITE ELEMENT ANALYSIS (FEA) OF MECHANISM

In order to examine stress distribution in the elements attached to the bolts, we performed FEA analysis on the plates connecting each of the three sections of the mechanisms (see Figure 16 for reference). The combination of plate materials is Glass Fiber/PLA, PLA/PLA and PLA/PLA in the order respectively. Each of the plates is subjected to an external load equal to weight of the mechanism components supported under it. Following material properties for materials are used in the simulation:

Table 3: Loading conditions for Analysis

Section	Load (N)	Torque (Nm)
Glass Fiber/PLA Plates	8.87	--
PLA/PLA Plates (Middle)	3.21	--
PLA/PLA Plates (Bottom)	0.24	--
Shaft	--	0.01765

Table 4: Properties of PLA and Glass Fiber

Material	Tensile Strength (MPa)	Yield Strength (MPa)	Young's Modulus (GPa)	Density (g/cm³)	Poisson Ratio
Glass Fiber[18]	2050	--	85	0.26	0.23
PLA[19][20]	37	26.08	2.89	1.3	0.33

The results of the simulation are presented in the results section of the report.

CONTROL ALGORITHM:

The control system of the mechanism is an open-loop system as depicted in the diagram below (Figure 19)

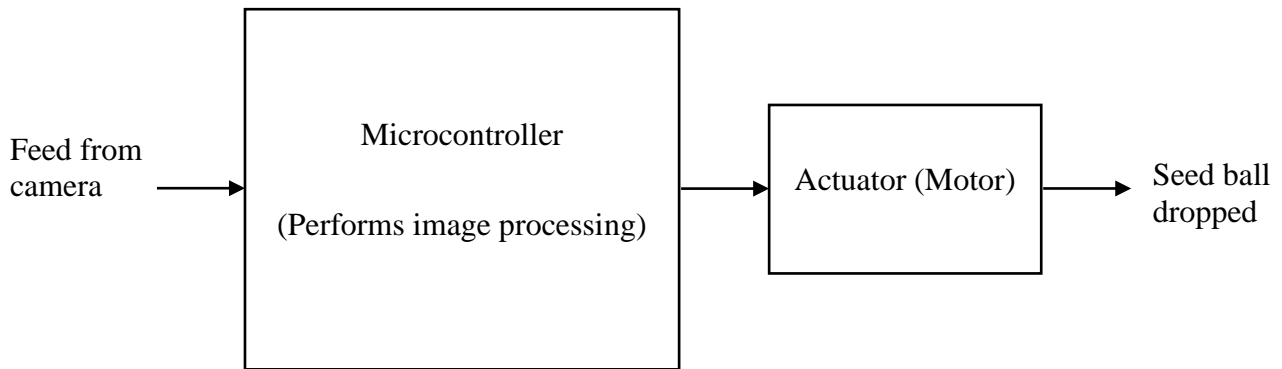


Figure 19: Control System Operation

The motor actuators which are responsible for the seed-balls' release from the mechanism are controlled by a raspberry pi microcontroller. The raspberry pi takes input from the live visual feed of the pi camera (attached to the Pi). The microcontroller captures a frame from the feed, applies the image processing algorithm and then based upon the results of that algorithm decides to actuate the motors.

The circuit diagram of the system is shown below. It consists of:

- 3 motors:
 - Circular containers are attached at the ends of the shafts of the motors which rotate the seed balls from the hopper above to the pipes below
 - The mechanism has the potential to drop seed balls in three directions i.e. vertically downwards, towards the left and towards the right. The 3 motors thus perform these independent tasks.
- Pi Camera
- Raspberry pi (microcontroller)

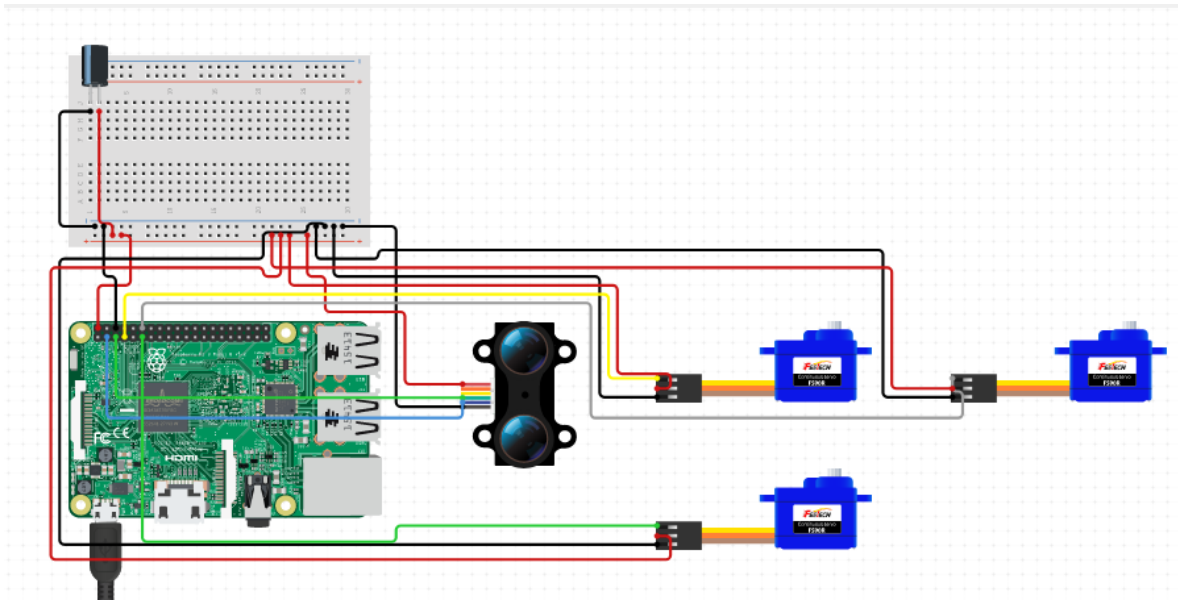


Figure 20: Circuit Design (made on Fritzing, an opensource circuit design software)

CHAPTER 4 RESULTS & CONCLUSIONS

CFD ANALYSIS

CFD analysis was performed on Simscale (an open source cloud computation package, which runs openFOAM on the backend). The incompressible, turbulent, steady state SIMPLE model was used, incorporating surface roughness of the tubing and Seedball. An inflation layer was applied to the surfaces of the Seedball and piping.

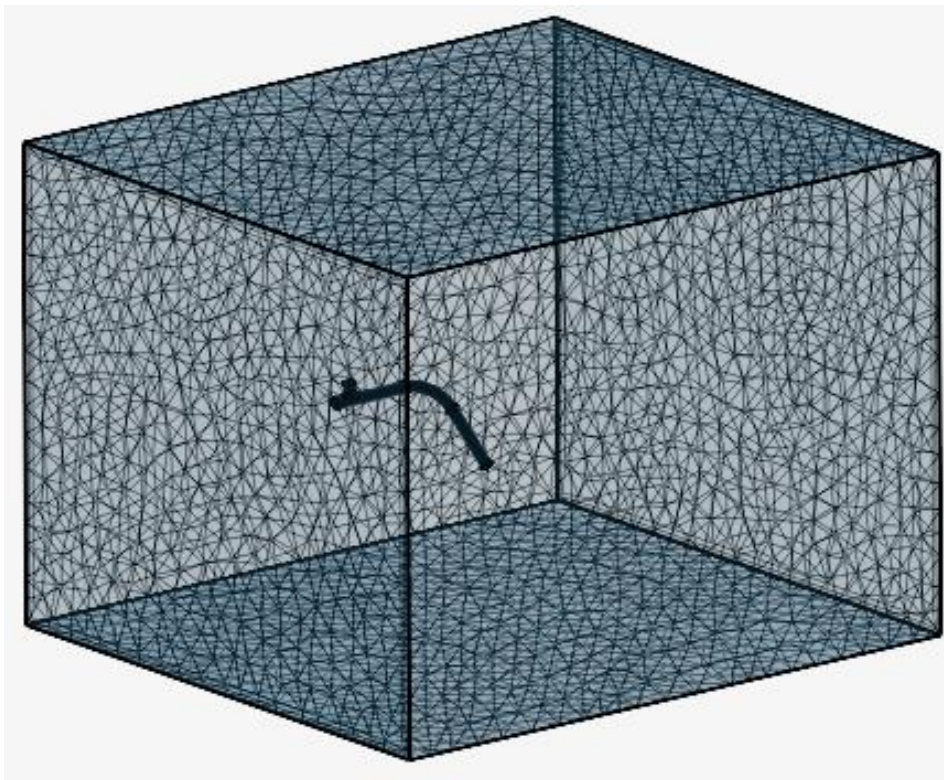


Figure 21: Meshing for the region around and inside Drop Ramp

The surface roughness parameters used were as follows:

$$\text{Roughness height (m)} = 1.1 \times 10^{-4} \text{ [21][22]}$$

$$\text{Roughness Constant} = 0.5$$

Velocity and the pressure profiles of the air inside the pipe with the ball placed inside (with and without the nozzle) were plotted. As can be clearly seen, the air forms a considerable pressure behind the ball which assists the ball movement. Through the CFD software, the drag coefficients and the pressure forces acting on the front side of the ball were found which have been shown below. The value of the pressure force was equivalent to the drag force calculated through $F_d = C_d * \frac{1}{2} * \rho * v^2 * A$ and hence we used this formula in our MATLAB simulation to incorporate the effect of wind force in our model. Drag coefficients were calculated at different locations in the pipe to get a realistic impact of wind on the ball. The results without the nozzle are shown below:

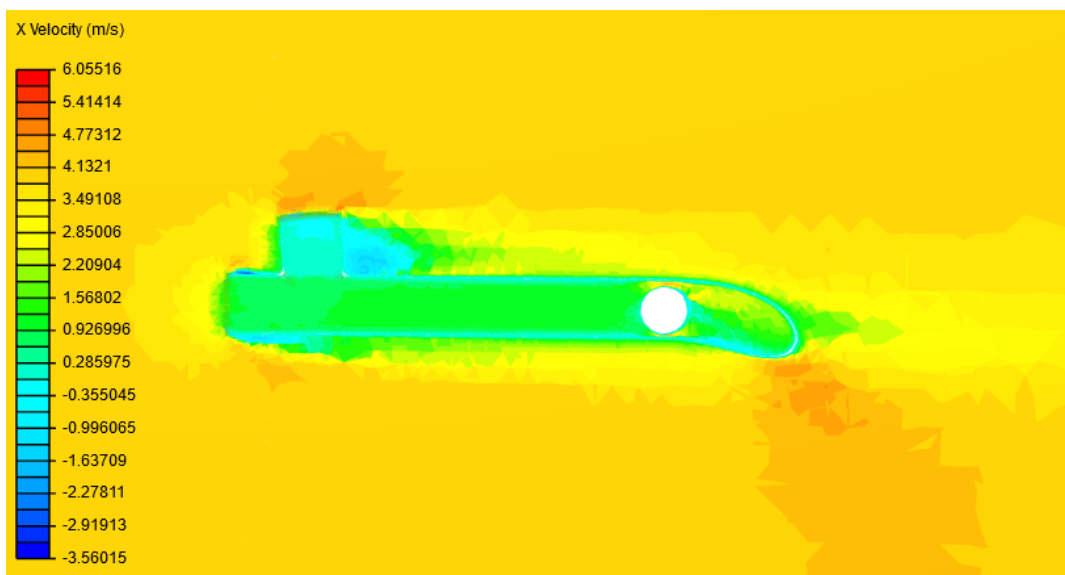


Figure 22: Velocity in x-axis for an Unnozzled Drop Ramp in a 4 m/s external flow field

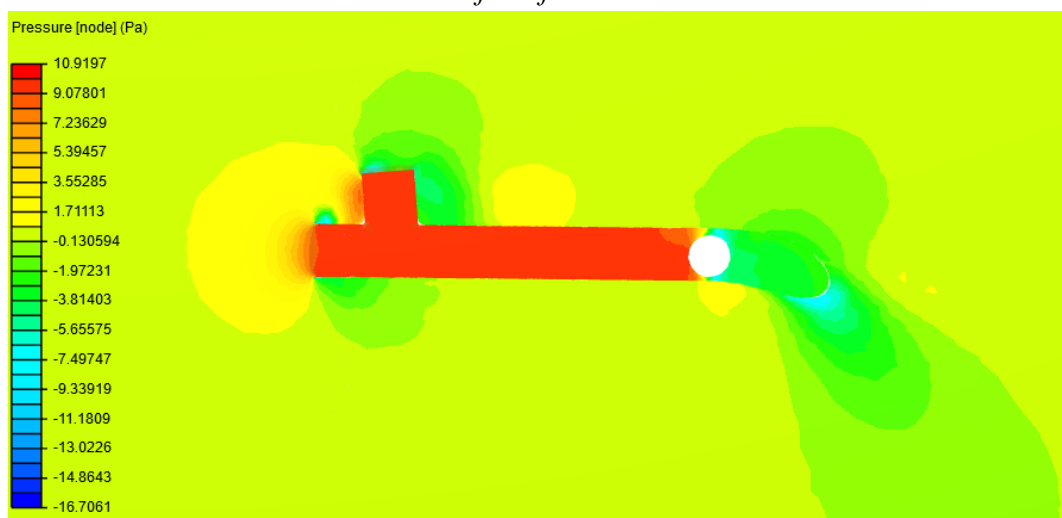


Figure 23: Pressure Distribution for an Unnozzled Drop Ramp in a 4 m/s external flow field

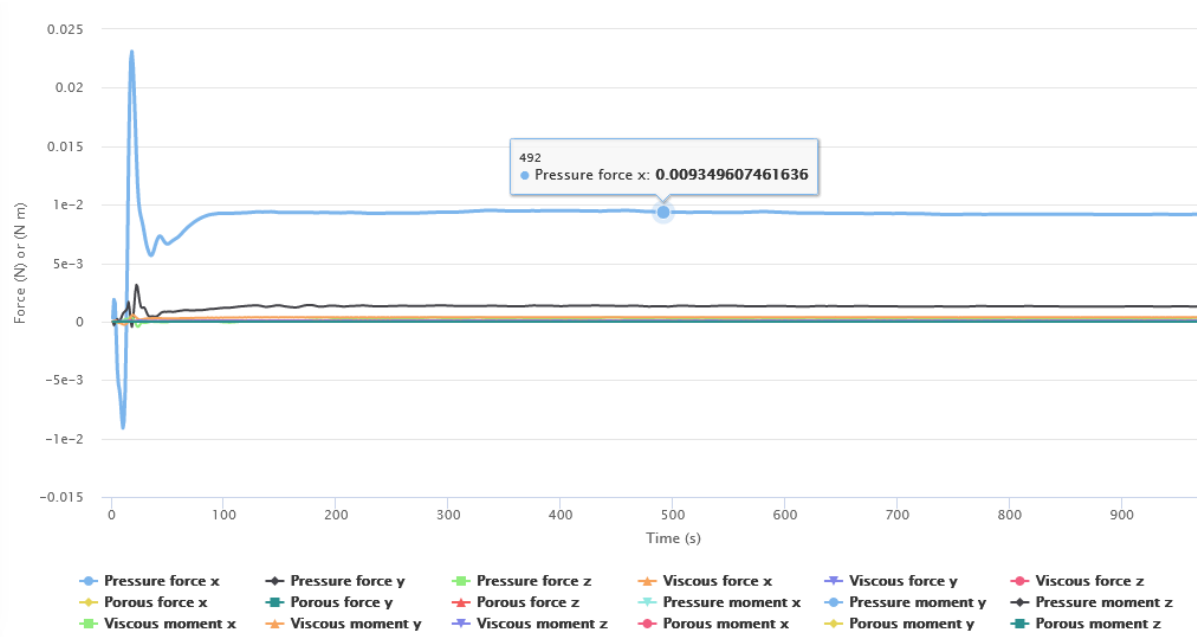


Figure 24: Force Coefficients convergence plot for Seedball in Unnozzled Drop Ramp

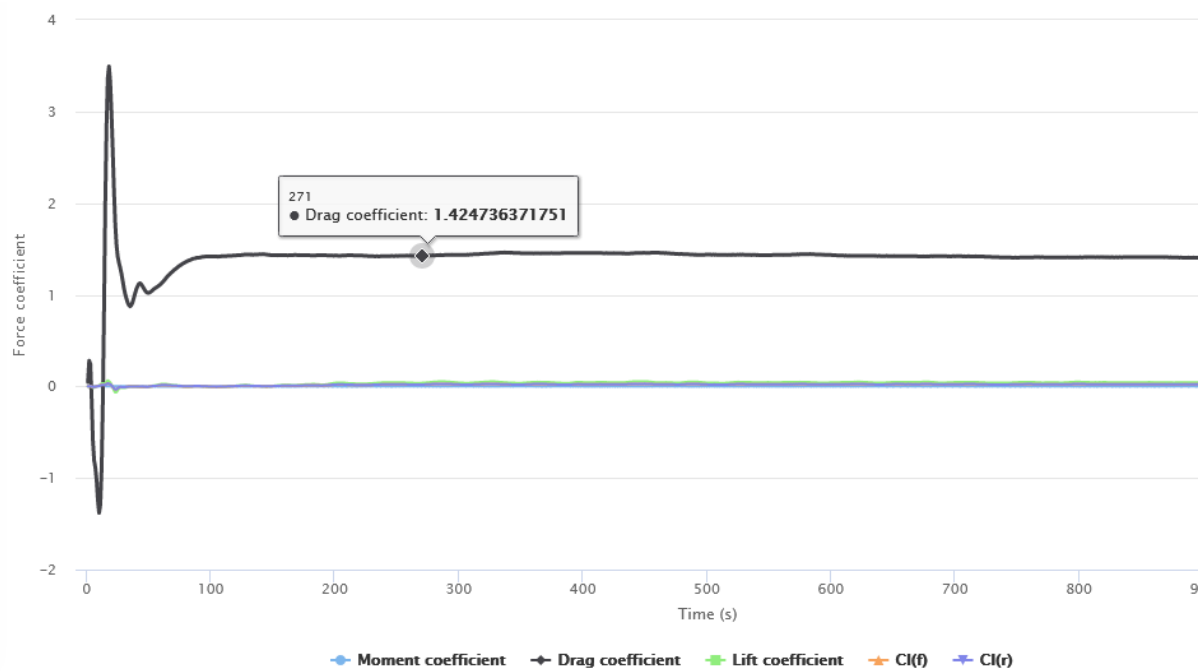


Figure 25: Force Convergence Plot for Seedball in Unnozzled Drop Ramp

In order to further increase drag on the Seedball, an attempt was made to increase the area of the air inlet. This was done by placing a nozzle on the air inlet.

$$\text{Air inlet area without nozzle} = 0.0007068 \text{ m}^2$$

$$\text{Air inlet area with nozzle} = 0.0050265 \text{ m}^2$$

Different variations of the nozzle were then added at the front of the pipe, all designed to minimize frictional losses. The results of the nozzle with minimal losses are shown below.

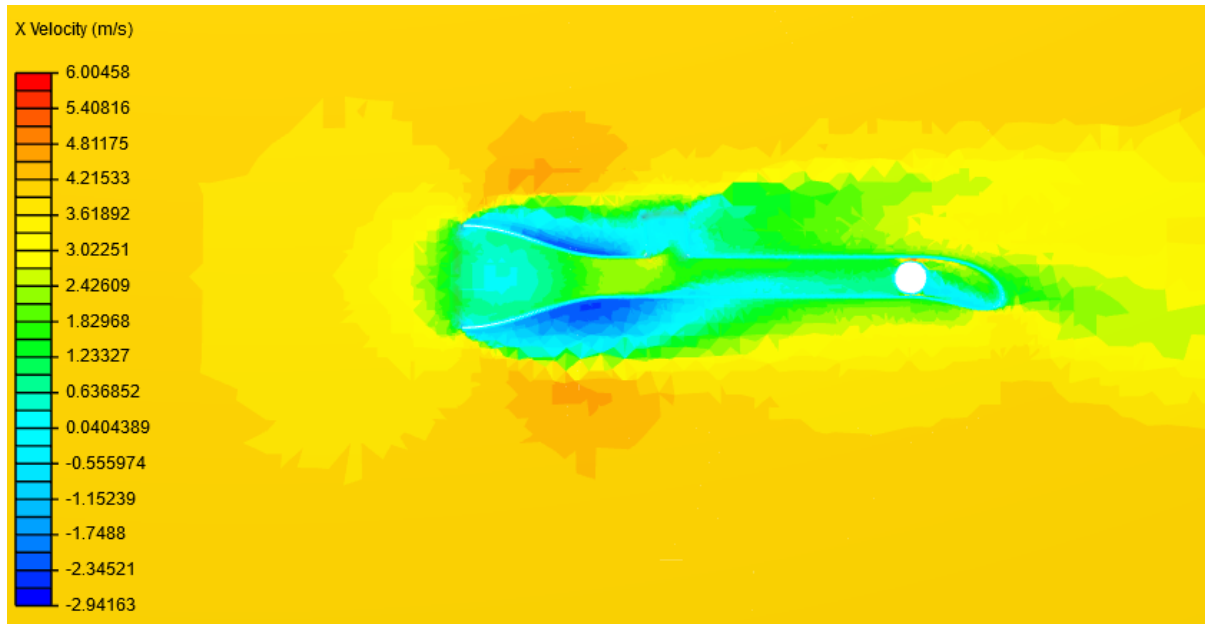


Figure 26: Velocity in x-axis for a Nozzled Drop Ramp in a 4 m/s external flow field

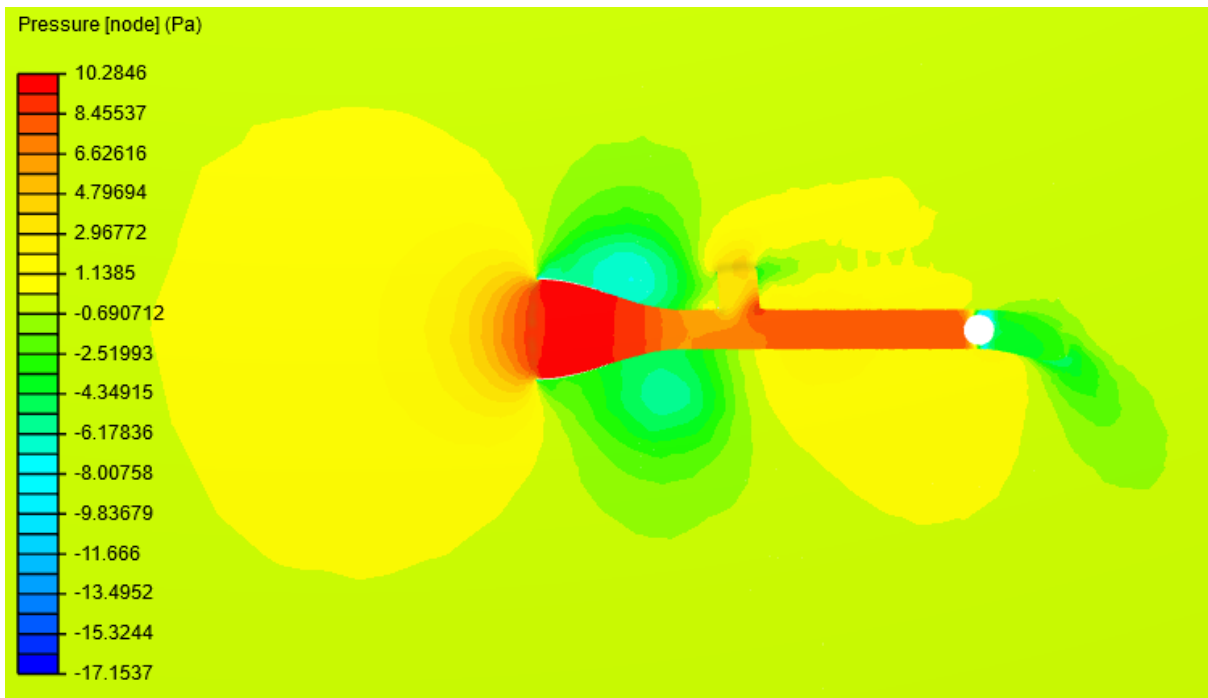


Figure 27: Pressure Distribution for a Nozzled Drop Ramp in a 4 m/s external flow field

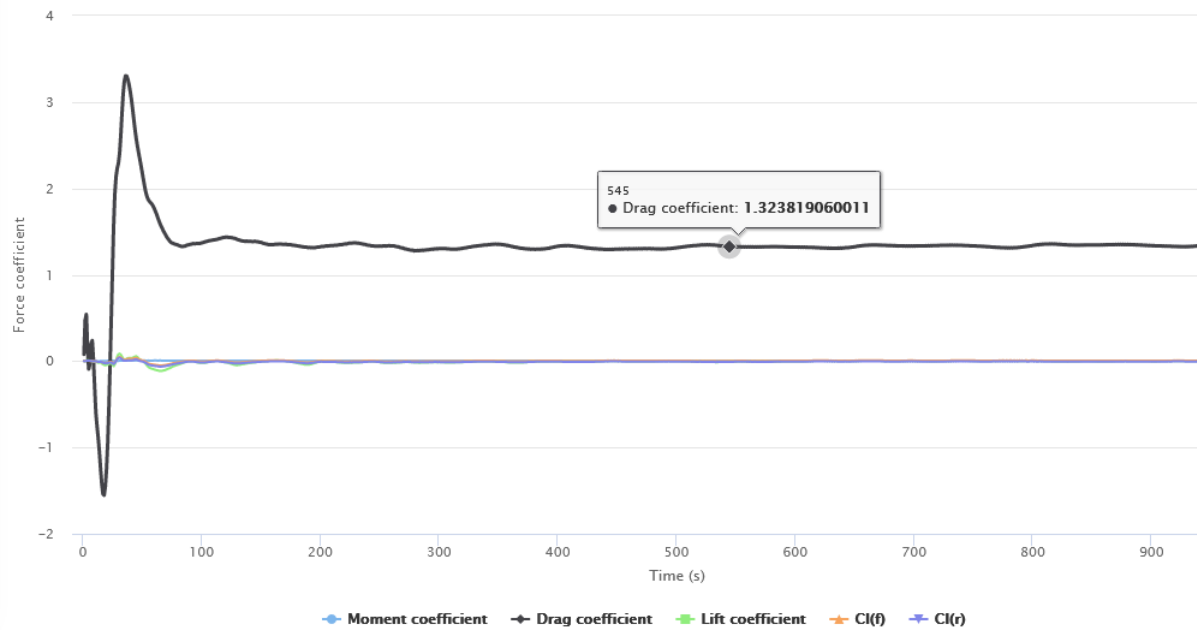


Figure 28: Force Coefficients convergence plot for Seedball in Nozzled Drop Ramp



Figure 29: Force convergence plot for Seedball in Nozzled Drop Ramp

The results of the simulation show that when we add a nozzle at the front of the pipe, the pressure build up behind the ball decreases resulting in a lower pushing force (as can be clearly seen from the Pressure force plot).

A seed ball was placed in different locations inside both piping networks (locations labelled A, B, C and D in figures below.) Drag forces and subsequently coefficients of drag were calculated. Averaged drag coefficients are tabulated below:

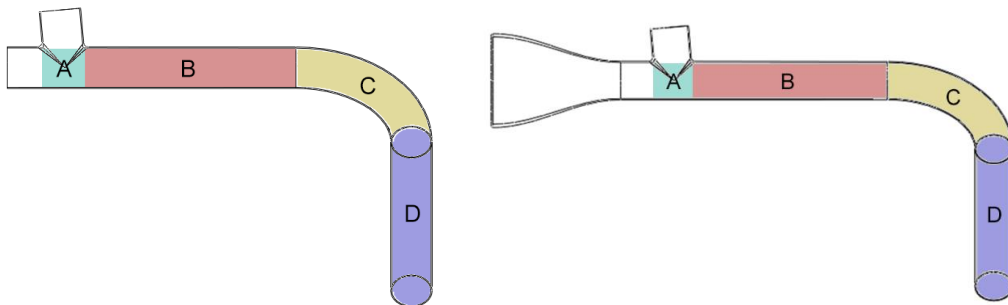


Figure 30: (A) Drop tube without nozzle (side view), (B) Drop tube with nozzle (side view). Note that wind inlet is through the opening on left hand side and Seedball enters tube through the opening at the top.

Table 5: Drag coefficients for both tubes for sections shown in Figure 30

Location in tube	Average coefficient of Drag (C_D)	
	No nozzle	With nozzle
A	1.0638	1.0343
B	1.4144	1.3055
C	1.4229	1.338
D	1.3392	1.3568

As clearly visible from the table, Coefficient of Drag was much lower for almost all pipe segments in the design with the nozzle. This translates directly to a lower force of air assistance as compared to the design without the nozzle. Since the design without the nozzle generated greater drag on the seed ball, this was finalized.

DRAG MODELLING

Having obtained coefficients of drag on the Seedball, the next step was to set up a simulation of the dynamic behavior of the system, incorporating the drag force on the Seedball:

$$F_{drag} = \frac{1}{2} C_D \rho A v^2$$

Dynamic modelling of the piping system was performed on MATLAB, using the SIMSCAPE Multibody Contact Forces Library. The piping after the point where the Seedball would fall into the drop ramp was simulated (See figure 28).

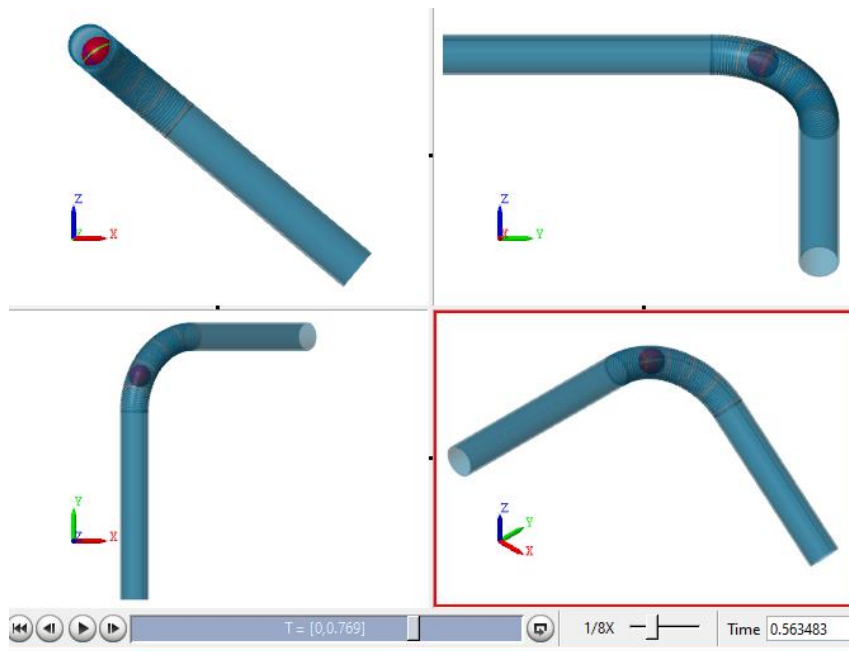


Figure 31: Multiple views of ball travelling through drop ramp in a SIMSCAPE Multibody Simulation

While the library is the most advanced software tool available for multibody contact simulation, limitations in its functionality only allow contact between a sphere and a straight tube to be modelled. Therefore, to model the bend, which was a curved tube, it was divided into 45 straight pipe segments, each rotated 2 degrees from the previous (see figure 32). This would allow very close approximation of a continuous 90-degree bend.

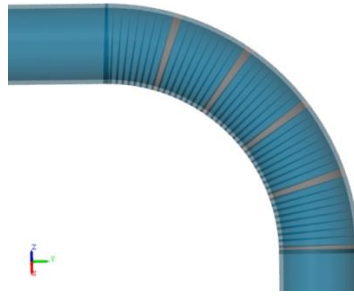


Figure 32: 90-degree bend in tube made using 45 differential segments

Inputting wind velocity into this model, we obtained values for:

1. Velocity of the Seedball upon exiting the mechanism.
2. Time taken for Seedball to exit the mechanism.

These were then input into the projectile motion model to calculate Seedball range at different altitudes for different wind velocities.

Both the MATLAB Code and the SIMSCAPE Block Network are given in Appendices III and IV respectively.

The results of the SIMSCAPE simulation for various wind speeds has been shown below:

Table 6: Ball Exit Velocities and time in tube for different wind velocities

Wind speed (m/s)	Ball exit velocity (m/s)	Time taken by ball (s)	% increase as compared to simple ramp ($V_{\text{exit}} = 1.489$ m/s for 25 cm ramp @ 40 degrees incline)
2	1.6594	1.9528	11.4
3	1.7399	1.4304	16.9
3.32	<i>1.7845</i>	<i>1.3182</i>	<i>19.8</i>
4	1.8619	1.0964	25.0
5	1.9860	0.9040	33.4
6	2.1202	0.7695	42.4

These test wind velocities were selected based upon the yearly wind speeds present in the Islamabad region. The average wind speed is 2.32 m/s[23] which when added to the drone speed of 1 m/s moving against the wind results in a net wind speed of the 3.32 m/s experienced by the seed ball.

PARAMETRIC ANALYSIS

Projectile Motion:

In order to select an optimal ramp angle for maximum horizontal displacement, the variation of the distance with the angle is studied using the projectile equations presented before. The study assumes a 4ms^{-1} relative velocity at an altitude of 8m. Following graph presents the results of the study

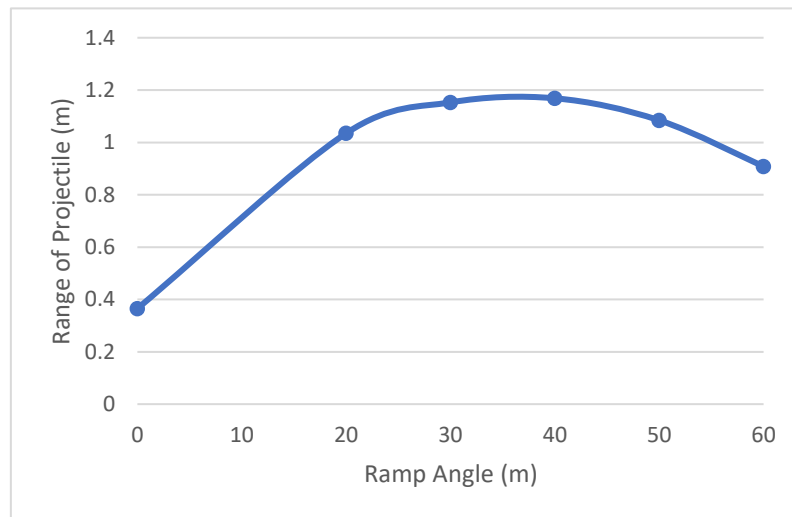


Figure 33: Relation of Ramp Angle and Range of Projectile

From the graph we can conclude

Maximum Range of the projectiles at 8m altitude = 1.1686m

Ramp angle = 40° below the horizontal

In order to demonstrate the effect of air induced force on horizontal range of the Seedball, we performed multiple simulations in our Simulink model which provided us with initial velocities of the Seedball at the exit of the pipe. Plugging these velocities in our projectile model, we can get the horizontal range at different altitudes. Following table represents the data:

Table 7: Effect of wind and altitude on projectile range

ALTITUDE (M)	6	8	10	12	14
WIND VELOCITY (MS ⁻¹)	Range (m)	Range (m)	Range (m)	Range (m)	Range (m)
2	1.3032	1.4518	1.6275	1.7834	1.9242
3	1.3329	1.5158	1.6999	1.8633	2.0109
3.32	1.33351	1.5517	1.7406	1.9082	2.0596
4	1.3842	1.6117	1.8085	1.9833	2.1410
5	1.4655	1.7079	1.9176	2.1039	2.2721
6	1.5519	1.8104	2.0343	2.2329	2.4122

We can see that increasing altitude and wind speeds have a remarkable effect on the range of the range of the drops.

MOTOR SELECTION

After calculating the torque on shaft with factor of safety of 5 we concluded to use *SG9g Mini Servo Motor* as it gives at least 3 to 4 times greater than required torque.

Required Torque = 0.18 kgcm

Torque obtained by selected motor = 0.6 kgcm

BEARING SELECTION

Radial load was calculated acting on the bearing and based on required reliability; we calculated basic dynamic load rating. Using SKF Catalogue; as required inner diameter of bearing was 5mm, we selected the *618/5 single row deep groove ball bearing*. This bearing provides more than 100 times required basic dynamic load rating as it is mentioned in calculations.

Required C_{10} = 2.84 N

C_{10} obtained from selected bearing = 468N

SHAFT ANALYSIS

Maximum shear stress was calculated acting on the shaft due to applied torque and it was compared to the tensile strength of material i.e. PLA used to manufacture shaft.

Maximum shear stress = 1.145 MPa

Tensile strength of PLA = 37 MPa

$$\text{Tensile Strength} > \text{Maximum shear stress}$$

As PLA is brittle so it cannot bend i.e. no bending load calculations required.

BOLT SELECTION AND ANALYSIS

Depending upon the thickness of members of joints, we selected standard size steel bolts for nonpermanent joint and checked whether these bolts could bear load acting on them. From calculations, it could be proved that all selected bolts can bear the external load easily as their calculated load factor is much greater than 1.

FINITE ELEMENT ANALYSIS

Since our loads are minimal compared to the strength of PLA and Glass Fiber, the resultant stresses in both materials are minimal. The stress plots top and bottom sides of each of the plate combinations can be seen in the following figures:

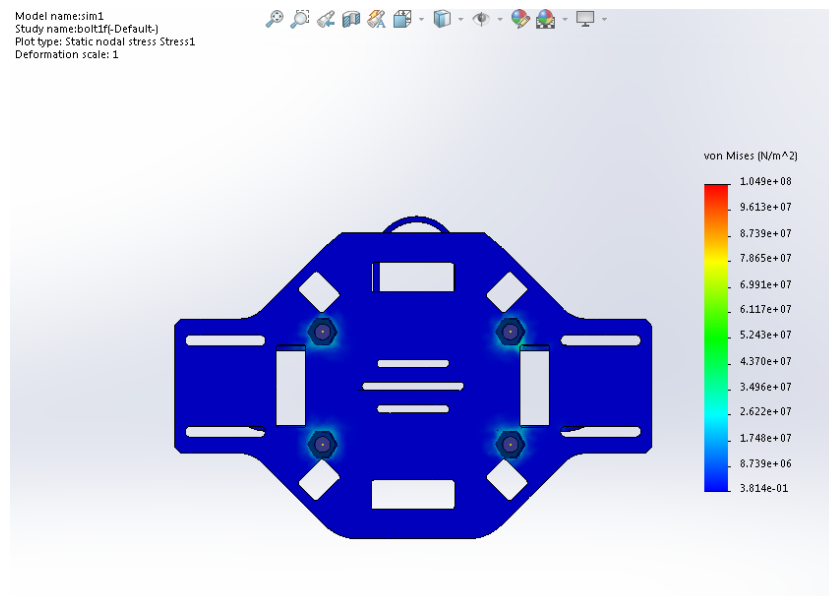


Figure 34: Glass Fiber/PLA Glass Fiber Side

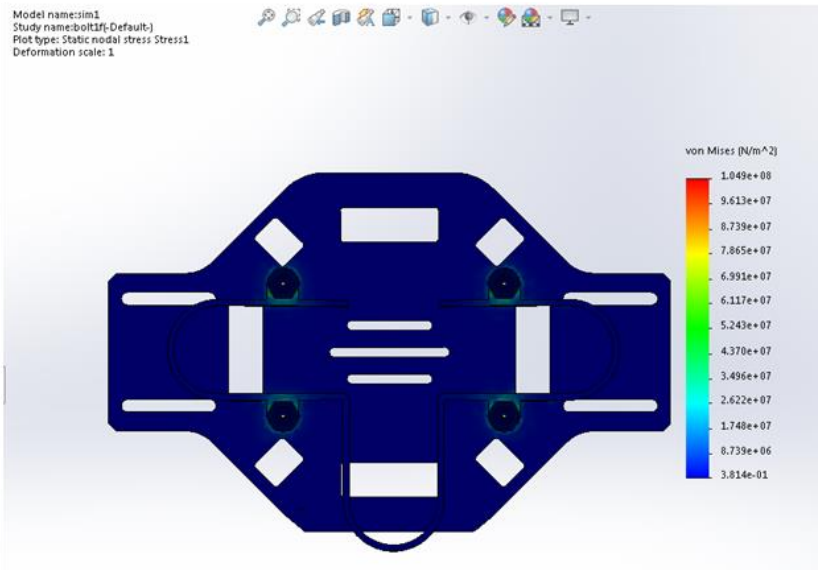


Figure 35: Glass Fiber/PLA Side

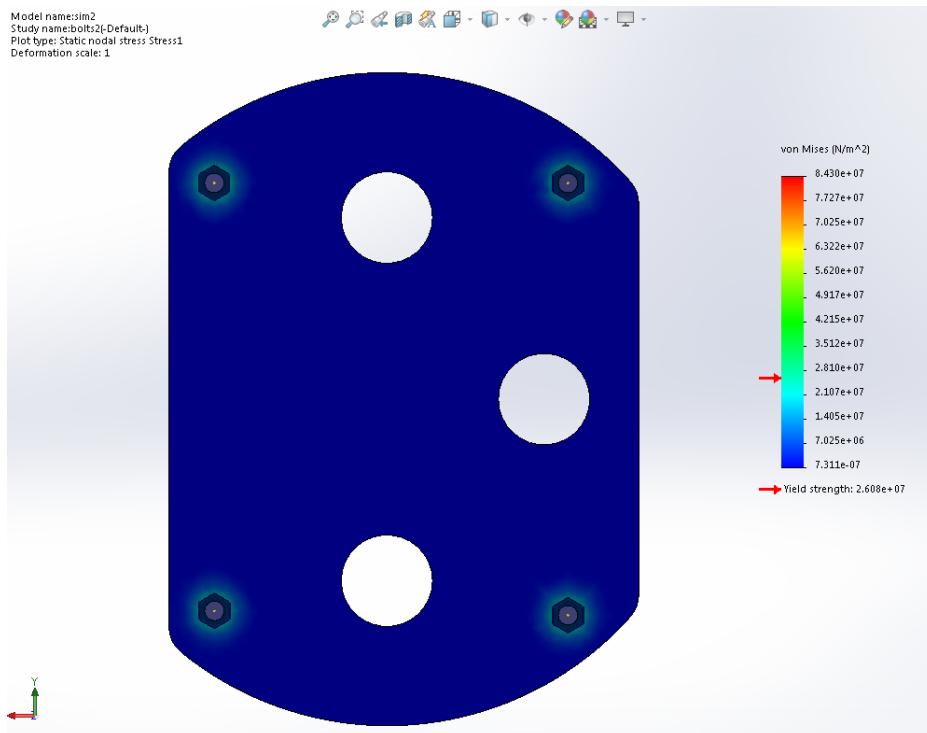


Figure 36: PLA/PLA Top Side

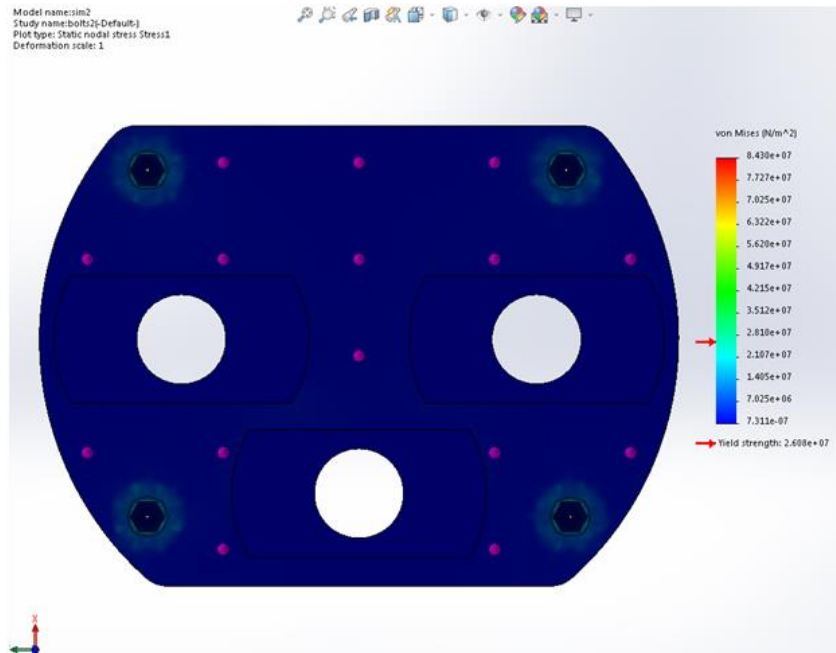


Figure 37: PLA/PLA Bottom Side

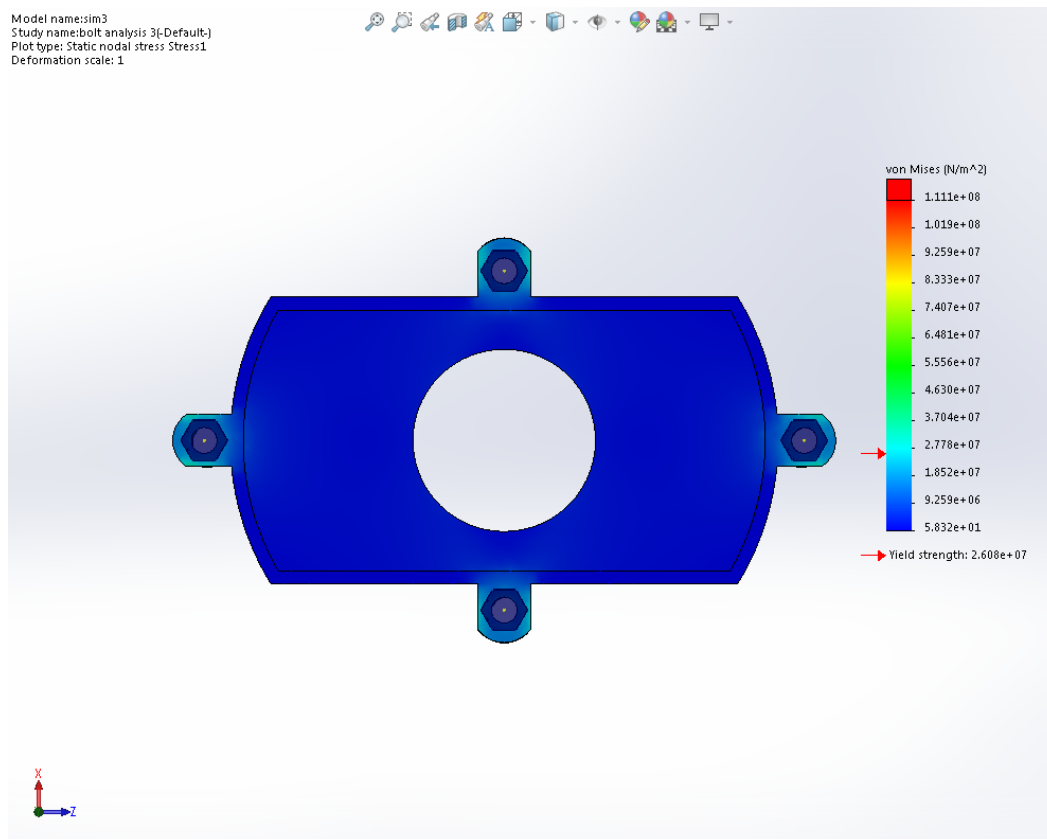


Figure 38: PLA/PLA Top (Bottom Section)

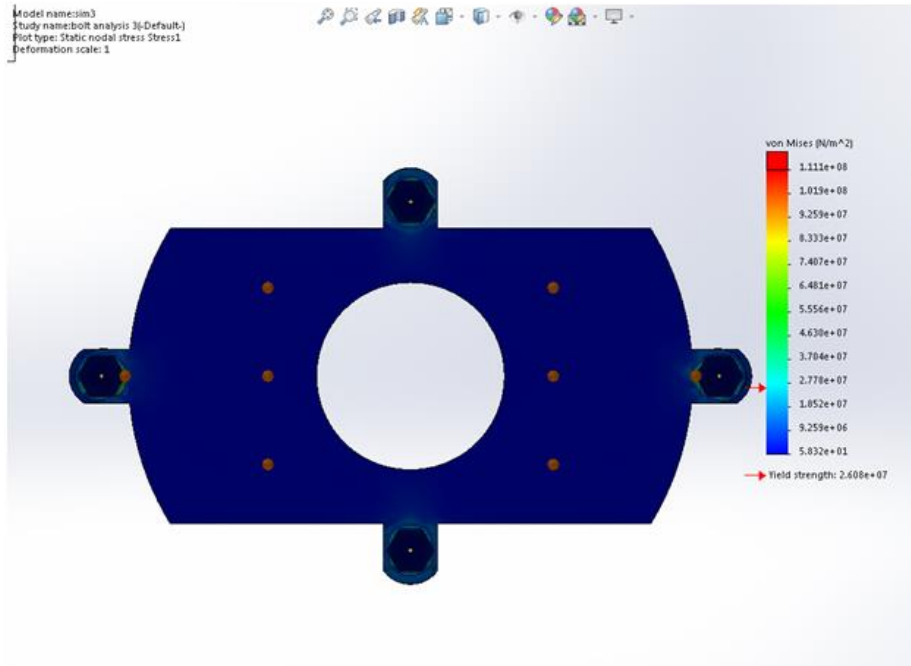


Figure 39: PLA/PLA Bottom (Bottom Section)

The following figure represents the stresses generated in the shaft under the effect of torque:

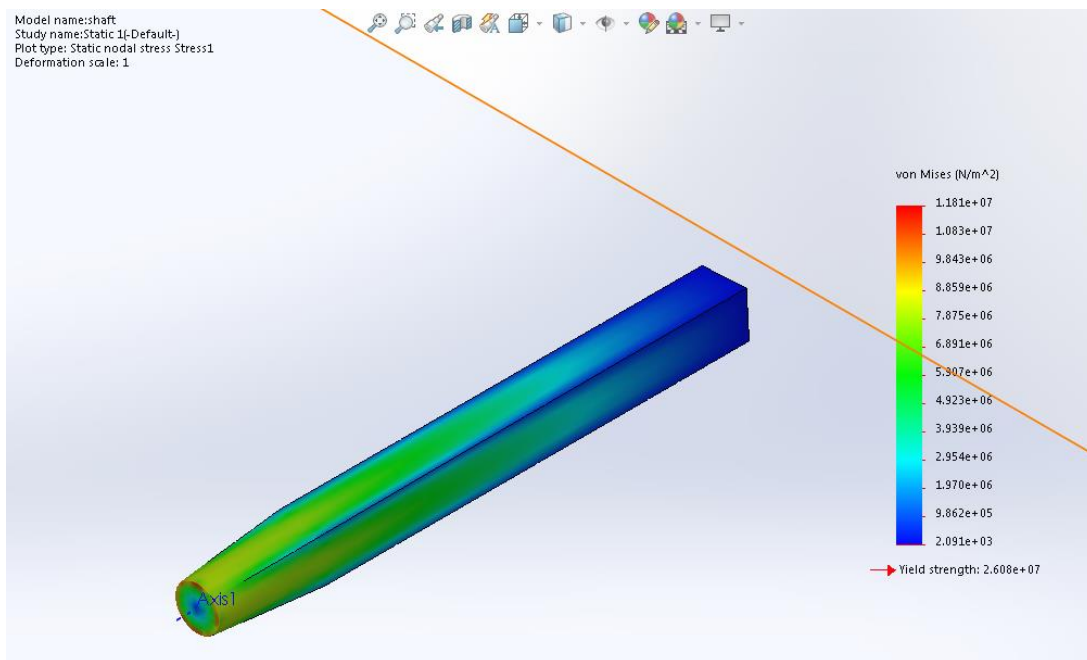


Figure 40: Stresses in Shaft

CONTROL ALGORITHM

The code was written in python and was uploaded in raspberry pi. The code first calls all the necessary libraries and then initializes the camera module and the motors. The code processes the frames obtained from the live feed using the PYTHON openCV library. The code divides the image into 3 parts (left, right and middle) and then a “mask” is added over the obtained images which separates out areas of plant able land. The microcontroller then determines if that area is above a certain threshold to actuate the appropriate motors. The total processing time taken by the raspberry pi to execute this algorithm is 0.3 seconds.

The code was tested on stock images obtained from the internet which resembled the actual operation conditions i.e. pictures taken from satellites and drones were used.

The image on the left is the frame which has been captured by the pi camera and the microcontroller then divides the photo into 3 parts as shown on the right image. Image processing algorithm is then run on each of these 3 parts separately and the results are shown below.

Areas marked by “white” color are the target areas where we need to plant the seed balls. The area marked by the “white” color is calculated by counting the number of white colored pixels and if that area is greater than a specified threshold, the microcontroller sends a command to actuate the motors to drop a seed ball in the required direction.



Figure 41: (A) Raw Image taken by PiCamera, (B) Image Split into thirds for image processing

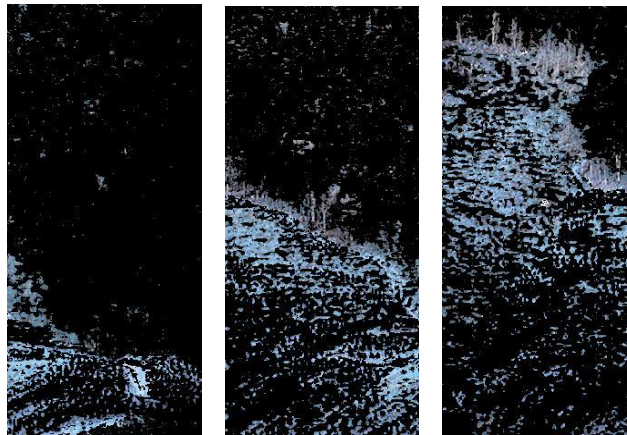


Figure 42: Results of Image Processing, (A) Left Third, (B) Central Third, and (C) Right Third

DRONE MOTION SIMULATION

Due to change in scope, instead of on ground testing, we simulated the drone using Software In The Loop (SITL) module of ArduPilot to monitor drone flight through a given set of waypoints. One of the objectives of the simulation was to get the pitch angle of drone which was used in pipe design.

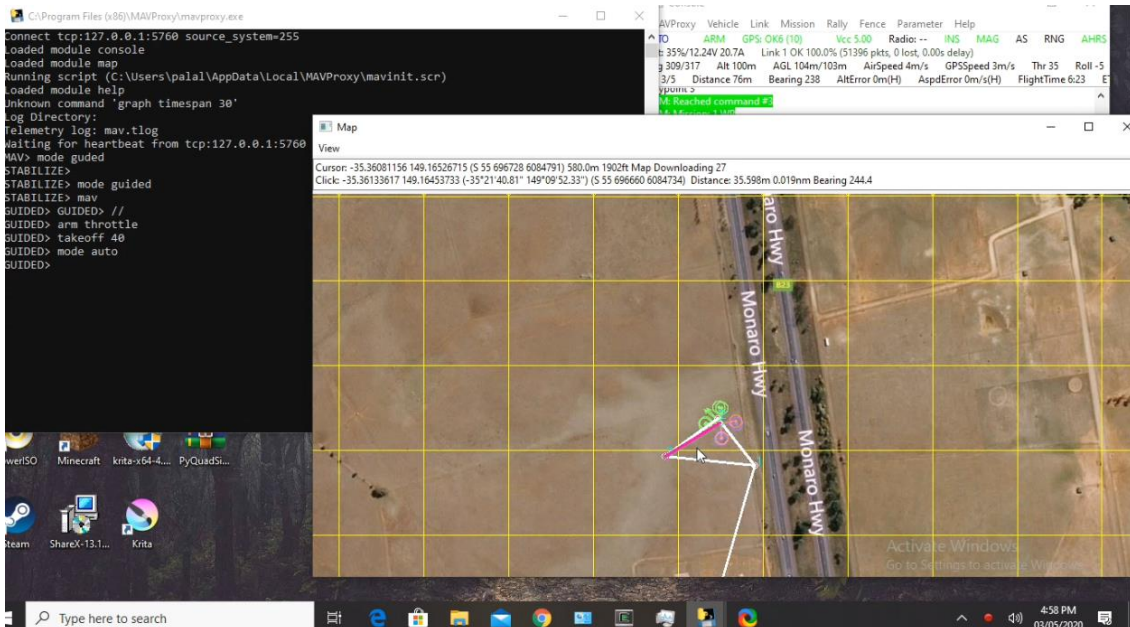


Figure 43: : Simulating a drone flight path on SITL on ArduPilot

CHAPTER 5 CONCLUSION & RECOMMENDATIONS

The project accomplished following objectives:

1. Design of a unique mechanism for dispersing Seedballs using quadcopters.
2. Mechanical analysis of the mechanism
3. Harnessing wind force to assist the drop of Seedballs (by increasing range).
4. Optimizing design of drop pipes through extensive study of wind motion in PLA pipes, in contact with Seedballs, computation of drag forces and effect of nozzles.
5. Estimating range of projectiles using drag based iterative projectile code.
6. Development of a control system to actuate motors and its integration with image processing algorithm.
7. Simulation of drone flight to find pitch angle.

Following recommendations can be used as a starting point for future work:

- a. **Variable Pipe Opening:** We can add an adjustable nozzle/opening at the entrance of the pipe to change the horizontal displacement of the ball. If there is some obstacle at the pre-determined drop location, we can make slight variations in the projectile range using the wind speed by adjusting the air flow into the pipes via a nozzle.

$$s = v * \cos(40) * t \dots \dots \dots (1)$$

$$H = v * \sin(40) * t + 0.5 * a * t^2 \dots \dots \dots (2)$$

Substituting (1) in (2)

$$H = s * \tan(40) + .5 * 9.81 * (s/v * \cos(40))^2$$

$$(v * \cos(40))^2 = (.5 * 9.81 * s^2) / (H - s * \tan(40)) = A$$

$$v = \sec(40) * \text{sqrt}(A)$$

The processing algorithm will also be modified as:

Identify obstacles using image processing

Calculate the distance adjustments that need to be made & how much should the opening be opened / closed

Send appropriate commands to the pipe opening

- b. **Expanding to Drone Swarms:** The designed mechanism can be attached to various drones and with the use of swarm programming, these drones can be used to cover wide areas of plantation with precise drops. This expansion can offer competition to the standard fixed wing UAV seed drops.
- c. **Employing Motion Planning Techniques:** Since the mechanism is actuated by image processing, motion planning techniques can be incorporated into the algorithm. Based on the wind speed, wind direction and the waypoints, the algorithm can devise a fuel-efficient path for drone. A further improvement would be to incorporate the ability to change the path in real time according to wind conditions.

The novelty in the project opens multiple avenues of overlapping research in fields of motion planning, swarm techniques, fluid dynamics and mechanics.

REFERENCES

- [1] Germanwatch e.V., 2020, *Global Climate Risk Index*.
- [2] Raoul G. Fima, 2003, “US6516565B1 - Airborne Seed Pouch Delivery System.”
- [3] Wood, A. D., 1984, “Developing a Seed-Containing Dart and Aerial Delivery System for Forestry Applications,” *For. Chron.*
- [4] Şahin, M., and Yıldırım, M. T., 2011, “APPLICATION OF A FIXED-WING UNMANNED AERIAL VEHICLE (UAV) IN REFORESTATION OF LEBANON CEDAR,” *Ankara International Aerospace Conference, AIAC*.
- [5] Grossnickle, S., and Ivetić, V., 2017, “Direct Seeding in Reforestation – A Field Performance Review,” *REFORESTA*.
- [6] Ortolani, M., Avra, S., Gabriele, C., and Schirone Bartolomeo, 2015, “Aerial Reforestation by Seed Bombs,” *International Conference: Reforestation Challenges, Belgrade, Serbia, 3-6 June 2015*.
- [7] Castro, J., Leverkus, A. B., and Fuster, F., 2015, “A New Device to Foster Oak Forest Restoration via Seed Sowing,” *New For.*, **46**(5–6), pp. 919–929.
- [8] “CDA Tree Plantation Drive” [Online]. Available: http://www.cda.gov.pk/projects/environment/Tree_Plantation/. [Accessed: 23-Dec-2019].
- [9] “Spacing Recommendations” [Online]. Available: https://www.kansasforests.org/conservation_trees/careandtips/spacing.html. [Accessed: 15-Jun-2020].
- [10] Hoerner, Sighard, F., 1985, “Fluid Dynamic Lift - Practical Information on

- Aerodynamic and Hydrodynamic Lift,” NASA STI/Recon Tech. Rep. A.
- [11] Faraz, M., 2018, *Study of Projectile Motion with Air Resistance*.
- [12] “SG90 Servo Motor Data Sheet.”
- [13] “Ball and Roller Bearing Catalog - 2202” [Online]. Available:
<http://www.ntnamericas.com/en/brochures-and-literature/catalogs/164>. [Accessed: 15-Jun-2020].
- [14] Budynas, R., and Nisbett, J. K., 2015, *Shigley’s Mechanical Engineering Design*.
- [15] 2018, *SKF Rolling Bearings Catalogue*.
- [16] “Torsion in Solid Square Sections” [Online]. Available:
<https://amesweb.info/Torsion/Torsion-Square-Sections.aspx>. [Accessed: 15-Jun-2020].
- [17] “Bolt Depot - Metric Nut Size Table - Diameter and Height” [Online]. Available:
<https://www.boltdepot.com/fastener-information/nuts-washers/Metric-Nut-Dimensions.aspx>. [Accessed: 15-Jun-2020].
- [18] “Properties: E-Glass Fibre” [Online]. Available:
<https://www.azom.com/properties.aspx?ArticleID=764>. [Accessed: 15-Jun-2020].
- [19] “PLA vs. ABS: What’s the Difference? | 3D Hubs” [Online]. Available:
<https://www.3dhubs.com/knowledge-base/pla-vs-abs-whats-difference/>. [Accessed: 15-Jun-2020].
- [20] Subramaniam, S. R., Samykano, M., Selvamani, S. K., Ngui, W. K., Kadirgama, K., Sudhakar, K., and Idris, M. S., 2019, “Preliminary Investigations of Polylactic Acid (PLA) Properties,” *AIP Conference Proceedings*, American Institute of Physics Inc.
- [21] Adams, T., Grant, C., and Watson, H., 2012, “A Simple Algorithm to Relate Measured

Surface Roughness to Equivalent Sand-Grain Roughness,” Int. J. Mech. Eng. Mechatronics.

- [22] Pérez, M., Medina-Sánchez, G., García-Collado, A., Gupta, M., and Carou, D., 2018, “Surface Quality Enhancement of Fused Deposition Modeling (FDM) Printed Samples Based on the Selection of Critical Printing Parameters,” Materials (Basel).
- [23] “Average Weather in Islamabad, Pakistan, Year Round - Weather Spark” [Online]. Available: <https://weatherspark.com/y/107761/Average-Weather-in-Islamabad-Pakistan-Year-Round>. [Accessed: 15-Jun-2020].

APPENDIX I: IMAGE PROCESSING CODE

```
# import the necessary packages
from picamera.array import PiRGBArray
from picamera import PiCamera
import time
import cv2
import numpy as np #added new
import RPi.GPIO as GPIO

GPIO.setup(pin, GPIO.IN)
state=GPIO.input(pin)

#initialize motors

GPIO.setmode(GPIO.BOARD)
GPIO.setup(11,GPIO.OUT)
servo1 = GPIO.PWM(11,50)

GPIO.setmode(GPIO.BOARD)
GPIO.setup(13,GPIO.OUT)
servo2 = GPIO.PWM(13,50)

GPIO.setmode(GPIO.BOARD)
GPIO.setup(15,GPIO.OUT)
servo3 = GPIO.PWM(15,50)

servo1.start(0)
servo2.start(0)
servo3.start(0)

#initialize camera
camera = PiCamera()
camera.resolution = (640, 480)
camera.framerate = 2
rawCapture = PiRGBArray(camera, size=(640, 480))

# allow the camera to warmup
time.sleep(0.1)

#Image capture and processing

for frame in camera.capture_continuous(rawCapture, format="bgr",
    use_video_port=True):

# grab the raw NumPy array representing the image, then initialize the timestamp
# and occupied/unoccupied text

    image = frame.array

# Below code divides the obtained frame into 3 parts
    left = image[:480,:214]
```

```

mid = image[:480,213:427]
right = image[:480,427:]

#left

hsv_l = cv2.cvtColor(left, cv2.COLOR_BGR2HSV)

#Brown (Right side of hue spectrum)
mask1_l = cv2.inRange(hsv_l, (140,0,40), (180,250,255))
#Pink (Left side of hue spectrum)
mask2_l = cv2.inRange(hsv_l, (0,0,90), (14,75,255))
mask4_l = cv2.inRange(hsv_l, (0,0,85), (20,130,255))
#White/greyish stuff (Entire range except GREEN)
mask3_l = cv2.inRange(hsv_l,(80,0,100),(180,75,255))
mask_l = mask1_l + mask4_l + mask3_l + mask2_l
res_l = cv2.bitwise_and(left,left, mask= mask_l)

pixels_l = cv2.countNonZero(mask_l)

#mid

hsv_c = cv2.cvtColor(mid, cv2.COLOR_BGR2HSV)

#Brown (Right side of hue spectrum)
mask1_c = cv2.inRange(hsv_c, (140,0,40), (180,250,255))
#Pink (Left side of hue spectrum)
mask2_c = cv2.inRange(hsv_c, (0,0,90), (14,75,255))
mask4_c = cv2.inRange(hsv_c, (0,0,85), (20,130,255))
#White/greyish stuff (Entire range except GREEN)
mask3_c = cv2.inRange(hsv_c,(80,0,100),(180,75,255))
mask_c = mask1_c +mask4_c+ mask3_c + mask2_c
res_c = cv2.bitwise_and(mid,mid, mask= mask_c)

pixels_c = cv2.countNonZero(mask_c)

# right

hsv_r = cv2.cvtColor(right, cv2.COLOR_BGR2HSV)

#Brown (Right side of hue spectrum)
mask1_r = cv2.inRange(hsv_r, (140,0,40), (180,250,255))
#Pink (Left side of hue spectrum)
mask2_r = cv2.inRange(hsv_r, (0,0,90), (14,75,255))
mask4_r = cv2.inRange(hsv_r, (0,0,85), (20,130,255))
#White/greyish stuff (Entire range except GREEN)
mask3_r = cv2.inRange(hsv_r,(80,0,100),(180,75,255))
mask_r = mask1_r + mask4_r + mask3_r + mask2_r
res_r = cv2.bitwise_and(right,right, mask= mask_r)

pixels_r = cv2.countNonZero(mask_r)

#code for motor actuation

if pixels_l > 51200:
    servo1.ChangeDutyCycle(2)

```

```

if pixels_c > 51200:
    servo2.ChangeDutyCycle(2)

if pixels_r > 51200:
    servo3.ChangeDutyCycle(2)

    time.sleep(0.05)

if pixels_l > 51200:
    servo1.ChangeDutyCycle(12)

if pixels_c > 51200:
    servo2.ChangeDutyCycle(12)

if pixels_r > 51200:
    servo3.ChangeDutyCycle(12)

print ("waiting 0.5s")
    time.sleep(0.5)

if pixels_l > 51200:
    servo1.ChangeDutyCycle(2)

if pixels_c > 51200:
    servo2.ChangeDutyCycle(2)

if pixels_r > 51200:
    servo3.ChangeDutyCycle(2)

if pixels_l > 51200:
    servo1.ChangeDutyCycle(0)

if pixels_c > 51200:
    servo2.ChangeDutyCycle(0)

if pixels_r > 51200:
    servo3.ChangeDutyCycle(0)

    servo1.stop()
    servo2.stop()
    servo3.stop()
    GPIO.cleanup()

#clear the stream in preparation for the next frame

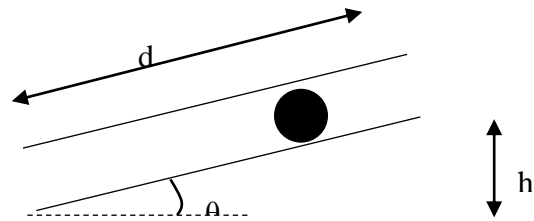
    rawCapture.truncate(0)

# if the `q` key was pressed, break from the loop

if key ==ord("q"):
    break

```

APPENDIX II: EXIT VELOCITY MODEL



Symbols:

- d = Pipe length
- h = Vertical component length of the inclined plane = $d * \sin(\theta)$
- θ = Angle of inclination of ramp
- m = mass of seed ball
- r = Radius of seed ball
- I = Moment of inertia of seed ball
- w = Angular velocity
- V_{ball} = Linear Ball velocity

The ball rolls in the pipes according to the following mathematical model:

$$\text{Energy in} = \text{Energy out}$$

$$\text{Gravitational potential energy} = \text{Friction} + \text{Linear K.E} + \text{Rotational K.E}$$

$$mgh = \frac{1}{2} * I * w^2 + \frac{1}{2} * m * V_{ball}^2$$

$$mgh = \frac{1}{2} * \left(\frac{2}{5} * m * r^2\right) * \left(\frac{V_{ball}}{r}\right)^2 + \frac{1}{2} * m * V_{ball}^2$$

$$mgh = V_{ball}^2 * \left(\frac{m}{5} + \frac{m}{2}\right)$$

$$V_{ball} = \sqrt{\frac{mgh}{\left(\frac{m}{5} + \frac{m}{2}\right)}}$$

$$V_{ball} = \sqrt{\frac{10}{7} * g * h}$$

APPENDIX III: MATLAB WORKSPACE VARIABLE DECLARATION

FOR SIMSCAPE MODEL

```
clear;
seedball.radius=0.015;
seedball.density=0.012/((4/3)*pi*seedball.radius^3);

wind.velocity=6;

tube_1.len=0.250;
tube_1.irad=0.017;
tube_1.orad=0.019;

diaofcurve=0.2;
theta=2;
no_of_segments=90/theta;

arclen=(pi*diaofcurve)/4;
transl=arclen/no_of_segments;

tube_3.len=transl+0.5*tube_1.irad*2*sind(theta);
tube_3.irad=0.017;
tube_3.orad=0.019;

tube_2.len=0.20;
tube_2.irad=0.017;
tube_2.orad=0.019;

%% Wind Velocity 2
% t1=0.2;
% t2=1.525;
% t3=1.6;
% t4=1.66;
% t5=1.71;
% t6=1.75;
% t7=1.79;
% sim_run_time=1.952846;

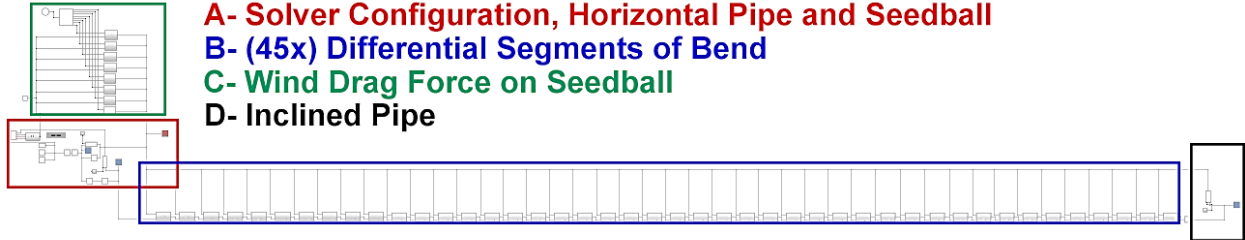
%% Wind Velocity 3
% t1=0.2;
% t2=1.05;
% t3=1.11;
% t4=1.165917;
% t5=1.214648;
% t6=1.26;
% t7=1.3;
% sim_run_time=1.430399;
%% Wind Velocity 3.32
% t1=0.2;
% t2=0.888083;
% t3=1.022285;
% t4=1.065508;
% t5=1.107984;
% t6=1.141646;
```

```
% t7=1.179491;
% sim_run_time=1.318202;

%% Wind Velocity 4
% t1=0.1;
% t2=0.77;
% t3=0.82;
% t4=0.87;
% t5=0.91;
% t6=0.95;
% t7=0.98;
% sim_run_time=1.096434;

%% Wind Velocity 5
% t1=0.08;
% t2=0.62;
% t3=0.655;
% t4=0.69;
% t5=0.715;
% t6=0.745;
% t7=0.77;
% sim_run_time=0.904008;
%% Wind Velocity 6
t1=0.06;
t2=0.515;
t3=0.542;
t4=0.571;
t5=0.595;
t6=0.635;
t7=0.655;
sim_run_time=0.769483;
%% Section Averaged Coefficients of Drag
Cd_1=1.0638;
Cd_2=1.4144;
Cd_3=1.4229;
Cd_4=1.3392;
```

APPENDIX IV: SIMSCAPE MODEL

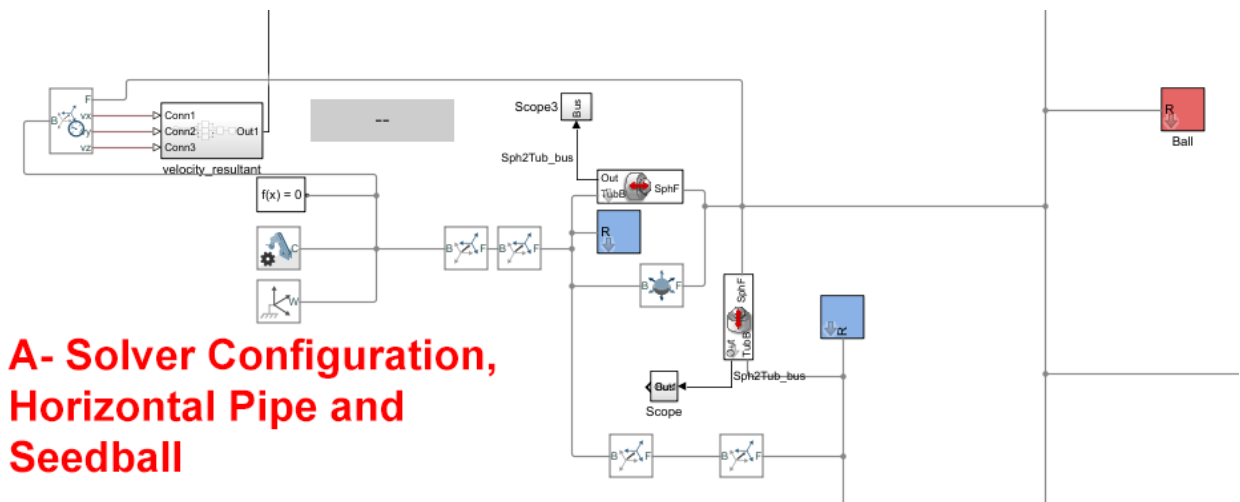


A- Solver Configuration, Horizontal Pipe and Seedball

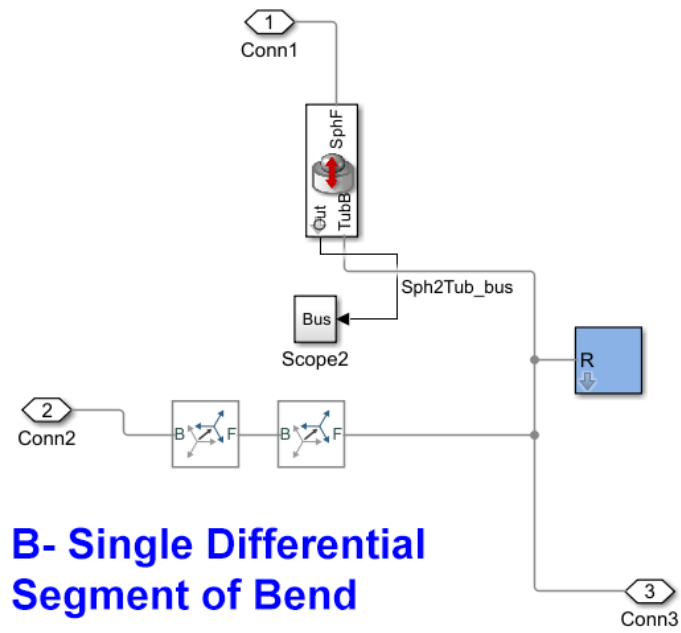
B- (45x) Differential Segments of Bend

C- Wind Drag Force on Seedball

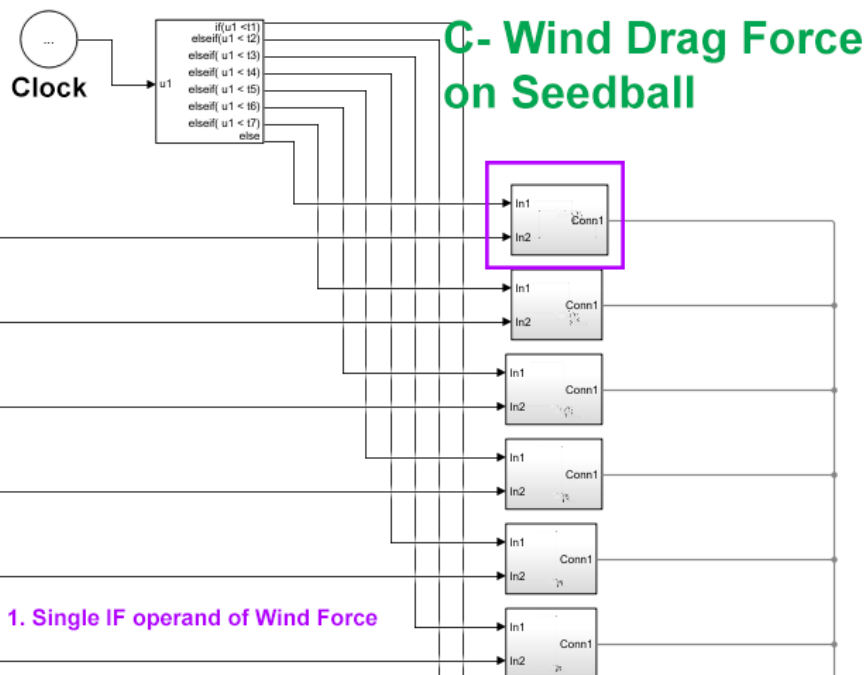
D- Inclined Pipe



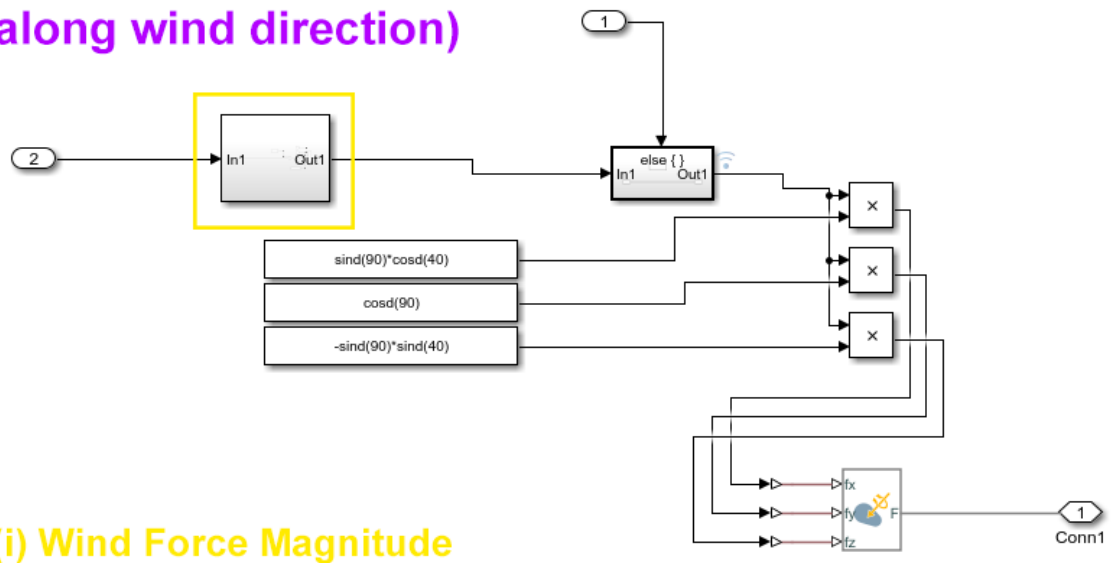
**A- Solver Configuration,
Horizontal Pipe and
Seedball**



B- Single Differential Segment of Bend

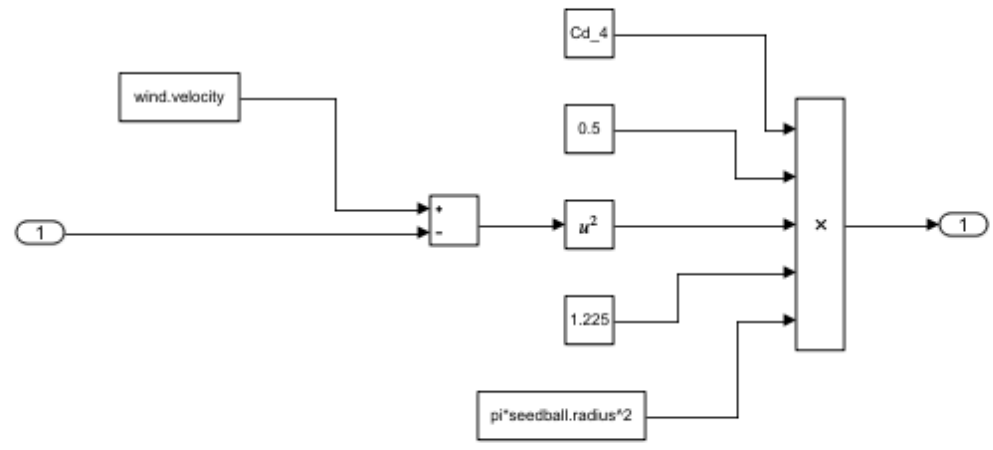


1. Single IF operand of Wind Force (Directing Force along wind direction)



(i) Wind Force Magnitude

(i) Wind Force Magnitude



D- Inclined Pipe

